

# รายงานวิจัยฉบับสมบูรณ์

## โครงการ

# การศึกษาคุณลักษณะเชิงของแข็งและการเปลี่ยนรูปของ นอร์ฟลอกซาซิน ไฮเดรต

## โดย

อาจารย์ เภสัชกรหญิง ดร. นฤพร สุตัณฑวิบูลย์ และคณะ

# รายงานวิจัยฉบับสมบูรณ์

### โครงการ

# การศึกษาคุณลักษณะเชิงของแข็งและการเปลี่ยนรูปของ นอร์ฟลอกซาซิน ไฮเดรต

คณะผู้วิจัย

1. อาจารย์ ภญ. ดร. นฤพร สุตัณฑวิบูลย์

2. Professor Stephen R. Byrn

3. เภสัชกร วันชัย จงเจริญ

สังกัด

ภาควิชาเภสัชอุตสาหกรรม

คณะเภสัชศาสตร์

จุฬาลงกรณ์มหาวิทยาลัย

Purdue University, USA

ภาควิชาเภสัชอุตสาหกรรม

คณะเภสัชศาสตร์

จุฬาลงกรณ์มหาวิทยาลัย

สนับสนุนโดยสำนักงานกองทุนสนับสนุนการวิจัย (ความเห็นในรายงานนี้เป็นของผู้วิจัย สกว. ไม่จำเป็นต้องเห็นด้วยเสมอไป)

#### กิตติกรรมประกาศ

คณะผู้วิจัยขอขอบคุณสำนักงานกองทุนสนับสนุนการวิจัย (สกว.) ที่ได้ให้การสนับสนุน เงินทุนวิจัยพื้นฐานแบบมุ่งเป้าหมาย "เคมีทางยา" ประจำปี 2548 สำหรับดำเนินการวิจัยในโครงการ "การศึกษาคุณลักษณะเชิงของแข็งและการเปลี่ยนรูปของนอร์ฟลอกซาซินไฮเดรต" ตามสัญญาเลขที่ DBG4880003 ทำให้งานวิจัยสำเร็จลุล่วงตามวัตถุประสงค์ทุกประการ

คณะผู้วิจัยใคร่ขอขอบคุณ ภาควิชาเภสัชอุตสาหกรรม (ปัจจุบันคือภาควิชาวิทยาการเภสัช กรรมและเภสัชอุตสาหกรรม) คณะเภสัชศาสตร์ จุฬาลงกรณ์มหาวิทยาลัย และ Purdue University ที่ได้ให้การสนับสนุนด้านบุคลากร เครื่องมือ และสถานที่การทำวิจัย

ที่สำคัญที่สุด คณะผู้วิจัยขอขอบคุณคณะกรรมการพิจารณาทุน รวมทั้งคณะกรรมการ ติดตามและประเมินผลงานวิจัย ที่ได้ให้ข้อเสนอแนะที่มีคุณค่าและเป็นประโยชน์อย่างยิ่งต่อการ พัฒนาและดำเนินการวิจัยในครั้งนี้ ให้ลุล่วงตามวัตถุประสงค์อย่างสมบูรณ์

คณะผู้วิจัย

#### บทคัดย่อ

รหัสโครงการ: DBG4880003

ชื่อโครงการ: การศึกษาคุณลักษณะเชิงของแข็งและการเปลี่ยนรูปของนอร์ฟลอกซาซิน

ไฮเดรต

**ชื่อนักวิจัย:** อาจารย์ ภญู. ดร. นฤพร สุตัณฑวิบูลย์

ภาควิชาเภสัชอุตสาหกรรม คณะเภสัชศาสตร์ จุฬาลงกรณ์มหาวิทยาลัย

Professor Stephen R. Byrn

Department of Industrial and Physical Pharmacy, Purdue University

ภก. วันชัย จงเจริญ

ภาควิชาเภสัชอุตสาหกรรม คณะเภสัชศาสตร์ จุฬาลงกรณ์มหาวิทยาลัย

E-mail Address: narueporn.s@chula.ac.th

ระยะเวลาโครงการ: 2 ปี

นอร์ฟลอกซาซินเกิดการจัดเรียงตัวในรูปไฮเดรต 4 แบบ (ไดไฮเดรต เฮมิเพนทะไฮเดร่ต ไตรไฮเดรต เพนทะไฮเดรต) และของแข็งอีกหนึ่งชนิดที่มีการจัดเรียงตัวอย่างไม่เป็นระเบียบ ไฮ เดรตทั้งหมดแสดงความเป็นผลึกเมื่อตรวจสอบด้วยการกระเจิงรังสีเอ็กซ์ นอร์ฟลอกซาซินไฮเดรท สามารถเกิดการเปลี่ยนรูปเป็นนอร์ฟลอกซาซินชนิดปราศจากน้ำรูปเอได้ภายใต้อุณหภูมิ 60 องศา เซลเซียสเป็นเวลา 48 ชั่วโมง ยกเว้นนอร์ฟลอกซาซินไดไฮเดรตและนอร์ฟลอกซาซินไตรไฮเดรตที่ พบโครงสร้างแบบผสม การลดความชื้นสัมพัทธ์เป็นศูนย์ไม่ทำให้เกิดการเปลี่ยนรูปของนอร์ฟลอก ซาซินชนิดปราศจากน้ำรูปเอได้อย่างสมบรูณ์ ผลของความร้อนทำให้นอร์ฟลอกซาซินไฮเดรต เปลี่ยนรูปแบบไม่สมบูรณ์ไปสู่ทรานสิชันนอลไฮเดรต ในขณะที่การลดความชื้นสัมพัทธ์ของนอร์ฟลอกซาซินเพนทะไฮเดรตทำให้เกิดการเปลี่ยนรูปไปสู่ของแข็งที่มีการจัดเรียงตัวอย่างไม่เป็น ระเบียบ ในสภาวะความชื้นสูงนอร์ฟลอกซาซินชนิดปราศจากน้ำรูปเอและชนิดไฮเดรต (ยกเว้นไดไฮ เดรต) เกิดการเปลี่ยนรูปเป็นนอร์ฟลอกซาซินเพนทะไฮเดรต โดยสรุปปัจจัยของความร้อน ความชื้นและเวลาที่สัมผัสต่างมีผลต่อการเปลี่ยนรูปของนอร์ฟลอกซาซินชนิดปราศจากน้ำรูปเอและ นอร์ฟลอกซาซินไฮเดรต

พลังงานดีไฮเดรชันของนอร์ฟลอกซาซินเฮมิเพนทะไฮเดรตมีค่าต่ำกว่าพลังงานดีไฮเดรชันของนอร์ฟลอกซาซินไตรไฮเดรตและนอร์ฟลอกซาซินเพนทะไฮเดรต ซึ่งเป็นผลอันเนื่องมาจากจำนวน ตำแหน่ง และความแข็งแรงของพันธะไฮโดรเจนที่เกิดขึ้นระหว่างโมเลกุล ของนอร์ฟลอกซาซินกับโมเลกุลของน้ำในโครงสร้างผลึก ปริมาณพลังงานทั้งหมดในการดีไฮเดรชันของนอร์ฟลอกซาซิน ไฮเดรตทั้งสามชนิด (เฮมิเพนทะไฮเดรต ไตรไฮเดรต และเพนทะไฮเดรต) ไม่ขึ้นกับอุณหภูมิไม่ว่าใช้วิธีการใดในการคำนวน สัมประสิทธิ์การจัดเรียงตัวของน้ำในโครงสร้างผลึกนอร์ฟลอกซาซินไดไฮเดรตมีค่ามาก แสดงว่าโมเลกุลของน้ำมีความพอดีกับช่องว่างในโครงสร้างผลึกนอร์ฟลอกซาซินไดไฮเดรตส่งผลให้มีช่องว่างอิสระในโครงสร้างผลึกน้อย ทำให้โครงสร้างผลึกนอร์ฟลอกซาซินยังคงความสมบูรณ์ได้ภายหลังจากการกำจัดโมเลกุลน้ำออก

คำหลัก: นอร์ฟลอกซาซินไฮเดรต, โครงสร้างผลึก, คุณลักษณะเชิงของแข็ง, การเปลี่ยนรูป,

พลังงานดีไฮเดรชัน

#### Abstract

Project Code: DBG4880003

Project Title: Solid State Characterization and Interconversion of Norfloxacin

Hydrates

**Investigator:** Narueporn Sutanthavibul, Ph.D.

Faculty of Pharmaceutical Sciences, Chulalongkorn University

Professor Stephen R. Byrn, Ph.D.

Department of Industrial and Physical Pharmacy, Purdue University

Wanchai Chongcharoen

Faculty of Pharmaceutical Sciences, Chulalongkorn University

E-mail Address: narueporn.s@chula.ac.th

Project Period: 2 years

Four stoichiometric norfloxacin (NF) hydrates (dihydrate, hemipentahydrate, trihydrate, pentahydrate) and one disordered NF state, were generated by various methods and characterized. X-ray powder diffraction (XRPD) patterns of all NF hydrates exhibited crystalline structures. NF hydrates transformed to anhydrous NF Form A after gentle heating at 60 °C for 48 hours except dihydrate and trihydrate where mixture in XRPD patterns between anhydrous NF Form A and former structures existed. Desiccation of NF hydrates at 0% RH for 7 days resulted in only partial removal of water molecules from the hydrated structures. The hydrated transitional phase and the disordered NF state were obtained from the incomplete dehydration of NF hydrates after thermal treatment and desiccation of pentahydrate NF, respectively. Anhydrous NF Form A and NF hydrates transformed to pentahydrate NF when exposed to high moisture environment except dihydrate. In conclusion, moisture levels, temperatures and duration of exposure influenced the interconversion pathways and stoichiometry of anhydrous NF and its hydrates.

NF hydrates did not show significant particle size reduction after dehydration due to the very compact structures and by high  $K_{chan}$  value obtained for dihydrate NF. Thus, NF hydrates were physically very stable and less likely to collapse after dehydration. Dehydration energy of lower stoichiometric hydrate (hemipentahydrate NF) was lower than higher hydrates (trihydrate NF and pentahydrate NF) due to the number, position and strength of hydrogen bonding between crystalline water and NF moiety in crystal lattice structure. The total dehydration energy for every NF hydrates were very high and found to be independent of temperature used.

**Keywords:** norfloxacin hydrate, crystal structure, interconversion, dehydration energy

## สารบัญ

	หน้า
กิตติกรรมประกาศ	ii
บทคัดย่อภาษาไทย	iii
บทคัดย่อภาษาอังกฤษ	iv
สารบัญ	٧
สารบัญรูป	vi
สารบัญตาราง	x
คำอธิบายสัญลักษณ์และคำย่อที่ใช้ในการวิจัย	xi
บทที่ 1 Introduction	1
บทที่ 2 Experimental	3
บทที่ 3 Results and Discussion	10
บทที่ 4 Conclusions	69
References	71
Appendices	77
บทที่ 5 ข้อเสนอแนะสำหรับงานวิจัยในอนาคต	83
Output จากโครงการวิจัย	84
ภาคผนวก	87

# สารบัญรูป

Figu	ure	หน้า
1	Model of IDSC thermogram of NF hydrate during isothermal dehydration	8
2	DSC and TGA thermograms of anhydrous NF Form A (A),	
_	disordered NF state (B), dihydrate NF (C), hemipentahydrate NF	
	(D), trihydrate NF (E) and pentahydrate NF (F)	11
3	Comparative HPLC chromatograms of various hydrates NF with	
0	standard NF in conjunction with the use of methyl paraben (MP)	
	as internal standard	13
4	XRPD patterns of anhydrous NF Form A (A), disordered NF state	13
7	(B), dihydrate NF (C), hemipentahydrate NF (D), trihydrate NF (E)	
	and pentahydrate NF (F)	14
5	HSM photomicrographs of NF hydrates immerse in mineral oil	14
J		
	upon heating (hemipentahydrate NF at ambient temperature (A), hemipentahydrate NF at temperarature over 120°C (B),	
	pentahydrate NF at ambient temperature (C), pentahydrate NF at temperarature over 120°C (D), dihydrate NF at ambient	
	. , , , ,	15
6	temperature (E), dihydrate NF at temperarature over 100°C (F))	15
6	Scanning electron photomicrographs of anhydrous NF Form A (A),	
	pentahydrate NF obtained from 100%RH vapor exposure (B) and	47
7	pentahydrate NF from directly dispersed in water (C)	17
1	Photomicrographs of anhydrous NF Form A after dispersed in	
	water at various contact time at the magnification of 400. (A. initial,	40
•	B. 15 minutes, C. 60 minutes and D.180 minutes)	18
8	DSC thermograms of disordered NF with respect to different	
_	heating temperature programs	20
9	XRPD patterns of disordered NF state (A), after D-I (B), after D-II	
	(C) and anhydrous NF Form A (D)	20
10	XRPD patterns of disordered NF states exposed to different	
	relative humidity for 7 days	21

11	FT-IR spectra of anhydrous NF Form A, disordered NF state and	
	other stoichiometric hydrates of NF	22
12	Dynamic water vapor moisture sorption and desorption isotherms	
	of anhydrous NF Form A at 25°C	23
13	XRPD patterns of anhydrous NF Form A under different relative	
	humidity for 7 days	25
14	XRPD patterns of dihydrate NF under 100% RH for 7 days	25
15	XRPD patterns of hemipentahydrate NF under desiccant (0% RH)	
	as a function of exposure time	26
16	XRPD patterns of trihydrate NF under desiccant (0% RH) as a	
	function of exposure time	27
17	XRPD patterns of anhydrous NF Form A (A), disordered state NF	
	(B), hemipentahydrate NF (C) and pentahydrate NF (D) after	
	heated at 60°C for 48 hours	28
18	XRPD patterns of dihydrate NF after heated at 60°C for various	
	time period	29
19	XRPD patterns of trihydrate NF after heated at 60°C for various	
	time period	29
20	Summary of the solid state interconversion of anhydrous NF Form	
	A and its hydrates	30
21	IDSC thermograms of hemipentahydrate NF during isothermal	
	dehydration at various T <sub>iso</sub>	31
22	XRPD diffractograms of dehydrated hemipentahydrate NF after	
	isothermal dehydration with respect to T <sub>iso</sub>	32
23	$\alpha\text{-t}$ curves of dehydration of hemipentahydrate NF at different $T_{iso}$	34
24	SEM photomicrographs of hemipentahydrate NF after complete	
	dehydration at various T <sub>iso</sub>	35
25	Comparative activation energy of dehydration derived from model	
	independent solid state kinetic of different stoichiometric NF	
	hydrates	36
26	IDSC thermograms of trihydrate NF during isothermal dehydration	
	at various T <sub>iso</sub>	37
27	IDSC thermograms of pentahydrate NF during isothermal	
	dehydration at various T <sub>iso</sub>	38

28	XRPD diffractograms of dehydrated trihydrate NF after first step of	
	isothermal dehydration with respect to T <sub>iso</sub>	41
29	XRPD diffractograms of dehydrated pentahydrate NF after first	
	step of isothermal dehydration with respect to $T_{\rm iso}$	42
30	XRPD diffractograms of dehydrated trihydrate NF after complete	
	dehydration with respect to T <sub>iso</sub>	43
31	XRPD diffractograms of dehydrated trihydrate NF after complete	
	dehydration with respect to T <sub>iso</sub>	44
32	SEM photomicrographs of dehydrated trihydrate NF during	
	isothermal dehydration after the first dehydration step with respect	
	to T <sub>iso</sub>	47
33	SEM photomicrographs of dehydrated pentahydrate NF during	
	isothermal dehydration after the first dehydration step with respect	
	to T <sub>iso</sub>	48
34	SEM photomicrographs of dehydrated trihydrate NF during	
	isothermal dehydration after the complete dehydration with respect	
	to T <sub>iso</sub>	49
35	SEM photomicrographs of dehydrated pentahydrate NF during	
	isothermal dehydration after the complete dehydration with respect	
	to T <sub>iso</sub>	50
36	$\alphat$ curves during dehydration of trihydrate NF at different $T_{\text{iso}}$	51
37	$\Omega\text{t}$ curves during dehydration of pentahydrate NF at different $T_{iso}$	51
38	The regular non isothermal DSC (NIDSC) thermograms of some	
	NF hydrates at the heating rate of 10 °C /min	54
39	Model of NIDSC thermogram (X to A) before IDSC thermorgram	
	(A to C) of NF hydrate during isothermal dehydration	54
40	The relationship between stoichiometry and dehydration energy of	
	NF hydrates obtained by different calculation methods (  IDSC	
	method alone, O regular NIDSC)	56
41	Photomicrographs of dihydrate NF during isothermal dehydration	
	at various T <sub>iso</sub> as a function of heating time	58
42	SEM photomicrographs of dihydrate NF after 360 mins of	
	isothermal dehydration with respect to different T <sub>iso</sub> .	59

43	The atomic positions of NF moiety and water of crystallization	
	molecules of dihydrate NF	62
44	The hydrogen bonding in crystal lattice of dihydrate NF structure	62
45	The crystallographic arrangement of water channel in dihydrate NF	
	structure along different unit cell axis (free red dots are crystalline	
	water)	64

## สารบัญตาราง

TABL	.E	Page
1	Water content (KF), percent weight loss (TGA) and stoichiometry	
	between NF and water molecules	12
2	Dehydration energy, residual water content and particle size of dehydrated	
	hemipentahydrate NF after complete dehydration at different	
	T <sub>iso</sub>	32
3	The activation energy of isothermal dehydration of hemipentahydrate NF	
	with various solid state kinetic models	36
4	Dehydration energy, residual water content and particle size of dehydrated	
	trihydrate NF after dehydration at different $T_{iso}$	39
5	Dehydration energy, residual water content and particle size of dehydrated	
	pentahydrate NF after dehydration at different $T_{iso}$	40
6	The activation energy of isothermal dehydration of trihydrate NF with various	
	solid state kinetic models	52
7	The activation energy of isothermal dehydration of pentahydrate NF with	
	various solid state kinetic models	52
8	The hydrogen bonds position and molecular property in dihydrate NF crystal	
	structure from crystallographic data	63
9	Crystal data of dihydrate NF	66
10	Crystallographic data of anhydrous NF Form A obtained from Powder	
	Indexing program of MATERIAL STUDIO® software simulated with XRPD $$	
	data	68

### คำอธิบายสัญลักษณ์และคำย่อที่ใช้

A pre exponential or frequency factor

AUC area under the curve

cm<sup>-1</sup> the reciprocal of cemtrimetre

et al. et alli, and others  $E_a$  activation energy

g gram

HPLC high performance liquid chromatography

J joule

k rate constant

 $K_{\text{chan}}$  the coefficient of packing

kJ kilo joule kV kilo voltage

In  $\alpha$  natural logarithm  $\alpha$  reacted fraction

mA milliampere
mg milligram
ml milliliter
min minute

r correlation of determination

mole

s second

mol

T absolute temperature

UV ultra violet

W watt

 $^{\circ}\text{C}$  degree centigrade  $^{\circ}2\theta$  degree of two theta

 $\mu$ I microlitre

%RH percentage relative humidity

w/v weight by volume w/w weight by weight

%T percentage transmission

### บทที่ 1

#### INTRODUCTION

Pharmaceutical manufacturing process plays an important role for new drug formulation development. One of the most significant processes in the pharmaceutical manufacturing procedure is drying operation. Drying can generally be achieved by employing either elevated temperature or reduced pressure. However, thermal drying is commonly used more than vacuum drying in industrial scale due to ease of operation. Regarding thermal drying, the solid phase conversion of materials may occur during dehydration (Byrn et al., 1999).

Proteins and peptides are well known for their thermal-labile property. Therefore, chemical properties of proteins often changed upon drying. Thermal dehydration of proteins eventually lead to stability problems and a failure in dosage form development (Abdul-Fattah, Kalonia and Pikal, 2007). Physical properties will also markedly be affected during dehydration such as cracks on the outer surface of particles can take place after thermal drying for some materials (Sakata, Shiraishi and Otsuka, 2004). Molecular adduct is an example which showed the solid state transformation during thermal dehydration. Ansolvate, a solvate without solvent molecules in the crystal structure, will be generated after the solvate is subjected to high temperature. The solvent molecule in the solvate is impeded as a result of the input energy from high temperature. Consequently, packing integrity of dehydrated materials will be altered and lead to structural weakness and finally structural collapse (Byrn et al., 1999). For example, drying of beclomethasone dipropionate monohydrate (BDM), antiasthmatic drug, resulted in the particle size reduction up to several folds after drying (Amolwan Chinapak, 2000). In addition, several groups of pharmaceutical solvates showed the same behavior as BDM where the particle sizes were reduced by desolvation. The removed solvent molecule from a solvate is a key factor to determine the extent of particle size reduction. This phenomenon has a complex behavior because the dehydration and size reduction occurred synchronously. The dehydration energy and the energy required to reduce the particle size of BDM are of great concern. Furthermore, different in stoichiometry of solvate/hydrate might determine the possibility of the particle size reduction by dehydration. Thus, it is important to study the relationship between molecular structures of solvate/hydrate and the dehydration energy required. In this study, norfloxacin (NF) is selected as model compound due to the versatility of stoichiometric

hydrates. It is necessary to determine the interconversion pathways amidst NF hydrates prior to evaluate the dehydration energy by thermal dehydration of the different stoichiometric NF hydrates.

### **Objectives of This Study**

- To crystallize and characterize solid state properties of various stoichiometry of NF hydrates
- To determine the interconversion pathways between various stoichiometric NF hydrates and anhydrous NF
- To evaluate energy required to induce the solid state interconversion between each stoichiometric NF hydrate and anhydrous NF

### บทที่ 2

#### **EXPERIMENTAL**

#### **CHEMICALS**

- Norfloxacin (anhydrous) Form A (Sigma Aldrich, USA)
- Isopropanol (IPA) (Mallinkrodt Chemicals, USA)
- Acetone (Mallinkrodt Chemicals, USA)
- Dichloromethane (Mallinkrodt Chemicals, USA)
- Ammonium hydroxide (J.T. Baker, USA)
- Hydrogen peroxide, 30% w/v (PanReac, Spain)
- Ortho-phosphoric acid (Univar, Australia)
- Lithium chloride, magnesium chloride, potassium carbonate, sodium bromide, sodium chloride, potassium bromide, potassium chloride, dextrose monohydrate, and potassium nitrate (Unilab, Australia)
- Anhydrous calcium sulfate (Drierite®, USA)
- Double distilled water

#### **INSTRUMENTS**

- Differential Scanning Calorimeter (822<sup>e</sup>, Mettler Toledo, Switzerland)
- Thermogravimetric Analyzer (TGA/SDTA851<sup>e</sup>, Mettler Toledo)
- Hot Stage (FP90, Mettler Toledo, Switzerland) equipped with optical microscope (Eclipse E2000, Nikon, Japan)
- Karl Fischer (720 KFS Titrino and 703 Ti Stand, Metrohm, Switzerland) with heating oven (KF 707, Metrohm, Switzerland)
- High Performance Liquid Chromatography (LC 10-ADvP, Shimadzu, Japan)
- X-ray Powder Diffractometer (D5000, Siemens, Germany)
- Scanning Electron Microscope (JSM-5410 LV, Jeol, Japan)
- Diffused ATR-Fourier Transformed Infrared Spectophotometer (Spectrum One® , Perkin Elmer, USA)
- Symmetrical Gravimetric Analyzer (SGA-100, VTI Corporation, Hialeah FL., USA).

#### **METHODS**

#### **Preparation of NF hydrates**

#### **Dihydrate NF**

Anhydrous NF Form A was dissolved in a mixture of IPA and water (0.915 mole fraction of IPA) at 60 °C in a light resistant container. The final NF concentration was equal to 1.5 mg/ml. The clear solution was allowed to cool down and left undisturbed at ambient condition to facilitate recrystallization. The resultant crystalline powder was harvested and kept in a tight and light-resistant container.

#### **Trihydrate NF**

Preparation of trihydrate NF was modified from the method reported by Puechagut et al. (1998). Anhydrous NF Form A was dissolved in 20% w/v aqueous ammonia solution to give a final clear solution at a concentration of 17.5 mg/ml. Antisolvent was obtained by mixing 564 ml of acetone and 156 ml of dichloromethane. The aqueous ammonia NF solution of 68.5 ml was gradually poured into antisolvent with continuous agitation. White and fluffy precipitates were developed and harvested. Dichloromethane was used to wash the resultant precipitates. The product was then placed in the drying oven at 50 °C for approximately 1 hour to remove residual solvents.

#### Hemipentahydrate and Pentahydrate NF

Hemipentahydrate NF and pentahydrate NF were prepared by hydration of anhydrous NF Form A at specified % RH level. Anhydrous NF Form A was placed under 75% RH and 100% RH at ambient temperature for 1 week to yield hemipentahydrate NF and pentahydrate NF, respectively (Katdare et al., 1986; Yuasa et al., 1982). Additionally, pentahydrate NF was also prepared by suspending anhydrous NF Form A in excess amount of double distilled water with continuous stirring. Dispersed solid was filtered and dried at ambient condition.

#### Solid state characterization of NF hydrates

#### Thermal analysis

The thermal properties of NF crystalline hydrates were evaluated using DSC with  $STAR^e$  software. Samples (5 mg) in aluminum pan with one pinhole were evaluated from 30-230  $^{\circ}C$  at a scanning rate of 10  $^{\circ}C/min$  under nitrogen purge at 60 ml/min.

TGA/SDTA was employed to investigate the liberation of volatile substance. The TGA operating conditions were the same as those used in the DSC study.

#### Hot stage microscopy (HSM)

HSM equipped with optical microscope was employed to evaluate solvates or hydrates (Vitez et al., 1998). Heating rate and temperature range were 10 °C/min and 30-240 °C, respectively. A small amount of sample was initially suspended in mineral oil and placed on a glass slide before being fixed on to the heating station. The liberation of gas bubbles at specified temperature was observed and recorded.

#### Karl Fischer titrimetry (KF)

The water contents of NF hydrates were monitored. Due to low solubility of NF hydrates in methanol, heating oven was selected as an additional attachment. Approximately 50 mg of the sample was inserted into the heating oven. The oven temperature of 160  $^{\circ}$ C was gradually increased to initiate the evaporation of water molecules. Water vapor was carried by dried nitrogen gas to react with KF reagents in the titration vessel where water contents were finally quantified.

#### X-ray Powder Diffraction (XRPD)

X-ray diffractometry was done with CuK $\alpha$  radiation at 40 kV and 20 mA. Samples were measured at a step size of 0.04 °2 $\theta$  with a scan speed 5 °2 $\theta$ /min from 5° to 35 °2 $\theta$ .

#### Fourier Transformed Infrared Spectroscopy (FT-IR)

ATR FT-IR was employed to observe the changes in peak position between anhydrous NF and NF hydrates. The samples were triturated and gently ground with dried potassium bromide in an agate mortar. The spectra were recorded as percent transmittance (%T) with respect to wave number ( $\nu$ ) in the range of 450 to 4000 cm<sup>-1</sup>.

#### Stability Indicating High Performance Liquid Chromatography (SI-HPLC)

SI-HPLC method was modified from the method used by Cordoba-Borrego et al.(1999). HPLC equipped with Hypersil BDS-C18 column in conjunction with C18-guard column was used. The mobile phase comprised of 0.1% v/v aqueous o-phosphoric acid:

acetonitrile at volume ratio of 70:30. The flow rate was equal to 1 ml/min. UV detection was carried out at 278 nm. Degradation product of NF was prepared by dispersing anhydrous NF in 30%w/v hydrogen peroxide in clear glass vial and was exposed to light and heat (80 °C) in an oven up to 8 hours. In addition, forced degradation in basic environment condition was evaluated according to the method used to prepare trihydrate NF. Small amount of anhydrous NF was added to 20% w/v aqueous ammonia solution and heated at 80 °C to initiate degradation.

#### Scanning Electron Microscopy (SEM)

The morphology of sample was recorded with a SEM at 15kV. The sample was carefully attached on the metal stub. It was then coated with gold by Sputter coater for 3 minutes at 0.05 mbar, 15mA with a working distance of 5 cm.

#### Solid State Interconversion of NF Hydrate

In an attempt to explore the interconversion pathways among NF hydrates and the anhydrous form, specific conditions were identified. Temperature and surrounding % RH were of main interest.

# Effect of Relative Humidity on the Conversion of Anhydrous NF and NF Hydrates

The effect of relative humidity on the conversion of anhydrous NF Form A was evaluated. Preliminary study on sorption and desorption behaviors of anhydrous phase was investigated by dynamic vapor sorption (DVS) using symmetrical gravimetric analyzer. Fifteen milligrams of anhydrous NF Form A was dried in a vacuum at 25  $^{\circ}$ C for 6 hours to minimize traces of surface associated water. Isothermic equilibrium condition of the cycle was 0.01% w/w within 15 min with a maximum step time of 75 min. The step change of % RH in both sorption and desorption phase were 5% RH/step. The change in sample weight against % RH was recorded.

Due to limited amounts of the samples obtained by DVS experiments, the sample at each equilibrium % RH was not sufficient to be collected in order to monitor for their solid state characteristics by XRPD. Thus, larger amounts of anhydrous NF Form A were exposed to specific moisture levels. The generation of various % RH in an air tight and light resistant container was made by using saturated solutions of lithium chloride (11.3% RH), magnesium chloride (32.8% RH), potassium carbonate (43% RH), sodium bromide

(57.5% RH), sodium chloride (75% RH), potassium bromide (81% RH), potassium chloride (84% RH), dextrose monohydrate (87% RH), potassium nitrate (93.7% RH) and purified water (100% RH) at 25  $^{\circ}$ C (Nyquist, 1983; Kotny and Conners, 2002). The sample powders were exposed to each relative humidity for 7 days before being characterized.

The preliminary results obtained by DVS and relative humidity exposures, indicated that phase transformation of anhydrous NF Form A to various stoichiometric hydrates occurred. Thus, every stoichiometric NF hydrate produced was subjected to an extreme moisture level of 100% RH and an extremely dry environment of 0% RH (Drierite®) and monitored for further transformation. The samples were stored for 7 days and then characterized by XRPD compared to the corresponding references. Additional storage time was needed in some cases where 7 days was insufficient to induce any changes in solid state transformation of NF hydrates.

#### **Effect of Temperature on the Conversion of NF Hydrates**

The temperature effect, particularly heating, was aimed to investigate dehydration of NF hydrates. A moderate temperature of 60 °C was selected in an attempt to avoid chemical degradation. NF hydrates were placed in the drying oven at 60 °C for 48 hours before being characterized by XRPD. However, additional exposure time up to one month was needed for some NF hydrates to confirm the solid state transformation.

#### **Isothermal Dehydration of NF Hydrates**

In order to control the effect of particle size on thermal dehydration, particle sizing was carried out with sieve analysis. The particle sizes of sample were in the range of 150 to 250 microns by using sieve No. 100 and No. 60, respectively.

Isothermal dehydration of NF hydrates was performed by isothermal DSC (IDSC). Four levels of isothermal dehydration temperatures ( $T_{iso}$ ) were 80 °C, 85 °C, 90 °C and 95 °C. Each sample was weighed approximately 20 mg and placed in aluminum pan (100  $\mu$ I) with manually pierced lid and sealed. It was then positioned onto DSC and the power level of DSC was monitored as a function of dehydration time ( $t_{iso}$ ). Nitrogen gas, with a flow rate of 60 ml/min, was purged into the system as a protective gas to prevent any possible oxidative reaction at high temperature.

From the preliminary test, the  $T_{iso}$  for different NF hydrates were varied depending on the nature of the hydrate structures. The results showed that trihydrate NF and pentahydrate NF consisted of two steps of dehydration. Thus, the solid samples for the

above NF hydrates were investigated at the end of each dehydration step. Unfortunately, hemipentahydrate NF did not show distinct steps of dehydration like trihydrate NF and pentahydrate NF. Therefore, the solid sample of hemipentahydrate was only obtained at the end of complete dehydration test.

The water content, particle size and crystal structure of dehydrated NF hydrates were measured by TGA, laser diffraction particle size analyzer and XRPD, respectively. The physical appearance of dehydrated sample was also observed with scanning electron microscope (SEM).

#### **Determination of Dehydration Energy of NF Hydrates**

Quantitative determination of energy used during dehydration was calculated based on the concept of the area under the curve (AUC) of IDSC thermogram. Total AUC obtained by trapezoidal rule from energy consumption-dehydration time profile was defined as the dehydration energy (Kishore, 1978). In addition, the determination of AUC of the dehydration of NF hydrate was specifically defined due to an uncommon IDSC thermogram seen from preliminary studies (Figure 1). During the early period of experiment, the power of IDSC was increase due to the equilibration of system (from point A to B). The later step from point B to C was an endothermic dehydration reaction. Thus, the extrapolation from point B to A' was additionally done and calculated as a part of the total AUC. Therefore, the total AUC was equivalent to the summation of the AUC of early stage of dehydration (from A' to B) and the AUC of the later stage of dehydration (from B to C).

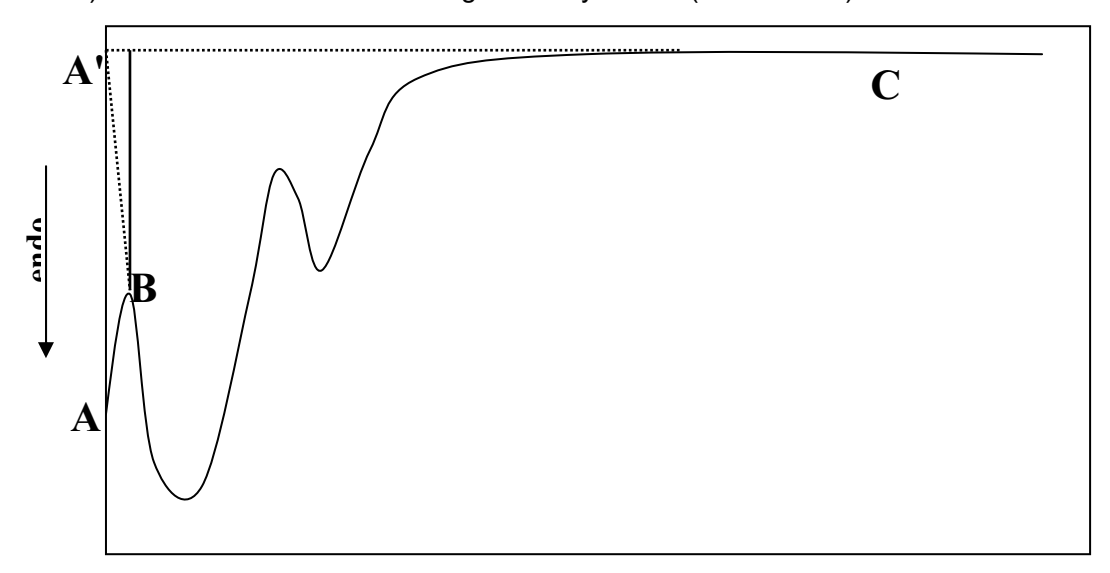


Figure 1 Model of IDSC thermogram of NF hydrate during isothermal dehydration

On the other hand, the calculation of activation energy ( $E_a$ ) for dehydration was determined by both model dependent and model independent solid state kinetic. Model dependent kinetic was determined from a plot of ln k from the solid state kinetic model versus reciprocal absolute temperature (1/T) provides  $E_a$  of dehydration from the slope ( $E_a/R$ ) (Byrn et al., 1999). Model independent kinetic, the slope from linear relationship of ln t and 1/T was calculated and resolved as  $E_a$  of dehydration (Dong et al., 2002 and Zhou et al., 2003).

### บทที่ 3

#### **RESULTS AND DISCUSSION**

#### **Solid State Characterization of NF Hydrates**

Anhydrous NF starting material was characterized by XRPD, DSC and TGA. TGA revealed negligible mass loss of less than 1% w/w which was in accordance with USP and BP specifications of anhydrous NF (USP 27; BP 2002). DSC and TGA thermograms of various NF forms are shown in Figure 2. DSC confirmed a single sharp endotherm at a temperature range of approximately 220 to 225 °C for anhydrous NF (Figure 2A). XRPD of anhydrous NF (Figure 4A) showed characteristic peak positions identical to those reported for NF Form A (Barbas et al., 2006; Katdare et al., 1986; Yuasa et al., 1982). It was hence concluded that the anhydrous NF in our experiment was polymorphic anhydrous NF Form A.

Slow recrystallization of NF solution in IPA:water mixture resulted in dihydrate NF. Thermal properties and water content of this hydrate are shown in Figure 2C. DSC and TGA thermograms showed endothermic peaks along with weight loss at the same temperature range of 80 to 140 °C. HSM also showed water vapor bubbles within the same temperature range (Figure 5F). Water content obtained by KF titration agreed well with the weight change obtained by TGA (Table 1) which indicated a stoichiometric dihydrate formation. XRPD pattern of the dihydrate NF was not reported in any previous publications for reference. Thus, a single crystal X-ray diffraction (SC-XRD) data from crystals obtained by the above recrystallization method was compared to NF dihydrate single crystal X-ray diffraction data reported by Florence et al. (2000) and were found to be identical. Therefore, the experimental XRPD pattern of NF dihydrate (Figure 4C) was confirmed by the calculated powder diffraction pattern generated from SC-XRD data by MERCURY software and served as reference XRPD pattern for dihydrate NF in future experiments. However, this recrystallization process was time-consuming and chemical degradation of NF is of great concern. The results obtained from SI-HPLC of the recrystallized NF dihydrate did not show degradation (Figure 3). Thus, the quality of NF dihydrate produced was essentially free from degraded compounds and was acceptable to be used as the reference for future studies.

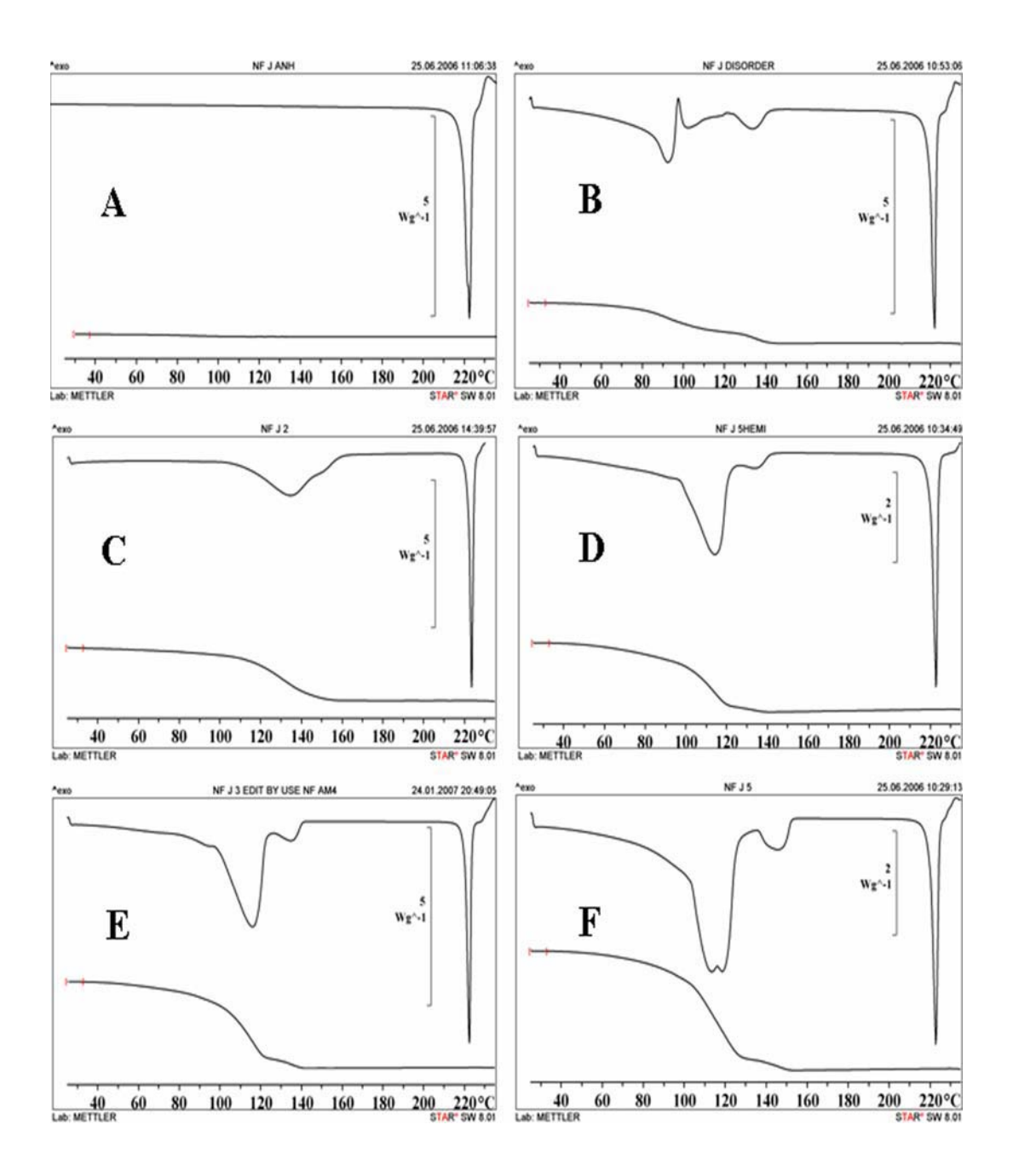


Figure 2 DSC and TGA thermograms of anhydrous NF Form A (A), disordered NF state (B), dihydrate NF (C), hemipentahydrate NF (D), trihydrate NF (E) and pentahydrate NF (F)

Table 1 Water content (KF), percent weight loss (TGA) and stoichiometry between NF and water molecules

Method of preparation	KF water content (%)	TGA % weight loss	Stoichiometry (NF:water molecule)
Desiccation NF pentahydrate	5.55(0.561)	6.24(0.372)	
Recrystallization from	10.10 (0.080)	9.34 (0.136)	1:2
IPA:water mixture			
Exposure to 75% RH	11.55 (0.611)	12.12 (0.039)	1:2.5
Precipitate from aqueous	14.49 (0.342)	14.81 (0.046)	1:3.0
ammonia solution			
Exposure to 100%RH	20.55 (0.367)	20.87 (0.153)	1:5.0

SD shown in parentheses.

Trihydrate NF generated from antisolvent precipitation was characterized. The results from HSM confirmed the existence of solvate or hydrate as seen from the evolution of vapor bubbles during heating. DSC yielded a large endotherm immediately followed by another minor endotherm at the temperature range of 80 to 130 °C (Figure 2E). Total weight loss obtained by TGA was 14.81% w/w and occurred at the same temperature range as that of the DSC endotherm (Figure 2E). Meanwhile, KF confirmed the trihydrate stoichiometry of the crystalline precipitate (Table 1). XRPD pattern shown in Figure 4E was used as reference XRPD pattern of trihydrate due to the fact that no reference XRPD pattern was available in any previous works. In addition, SI-HPLC did not detect any NF degradation after trihydrate NF was generated (Figure 3).

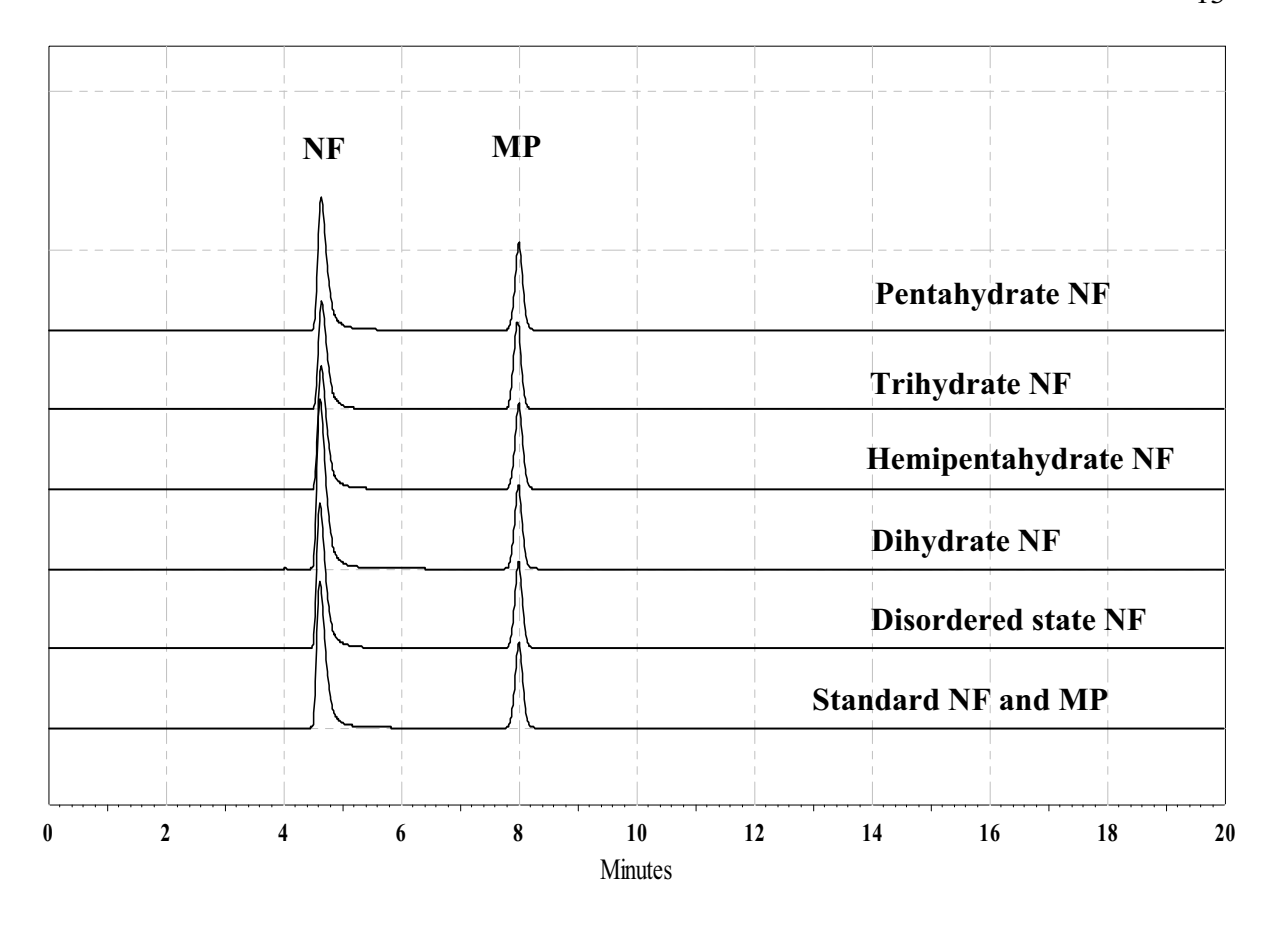


Figure 3 Comparative HPLC chromatograms of various hydrates NF with standard NF in conjunction with the use of methyl paraben (MP) as internal standard

DSC analysis of the hemipentahydrate NF (Figure 2D) and the pentahydrate NF (Figure 2F) which were produced from direct exposure to moisture, showed large endotherm followed by a smaller endotherm at approximately 120 °C and 140 °C, respectively. TGA showed a two step weight loss at the same temperature as achieved by DSC. The total weight loss from TGA and the water content obtained from KF were in good agreement confirming the stoichiometry of the hemipentahydrate NF and the pentahydrate NF (Table 1). HSM showed continuous liberation of vapor bubbles during the temperature ranges corresponding to their DSC and TGA dehydration endotherms (Figure 5A to 5D). XRPD of both hydrates are illustrated in Figure 4D and 4F and the XRPD patterns were essentially the same as XRPD of the hemipentahydrate NF and the pentahydrate NF reported by Yuasa et al (1982).

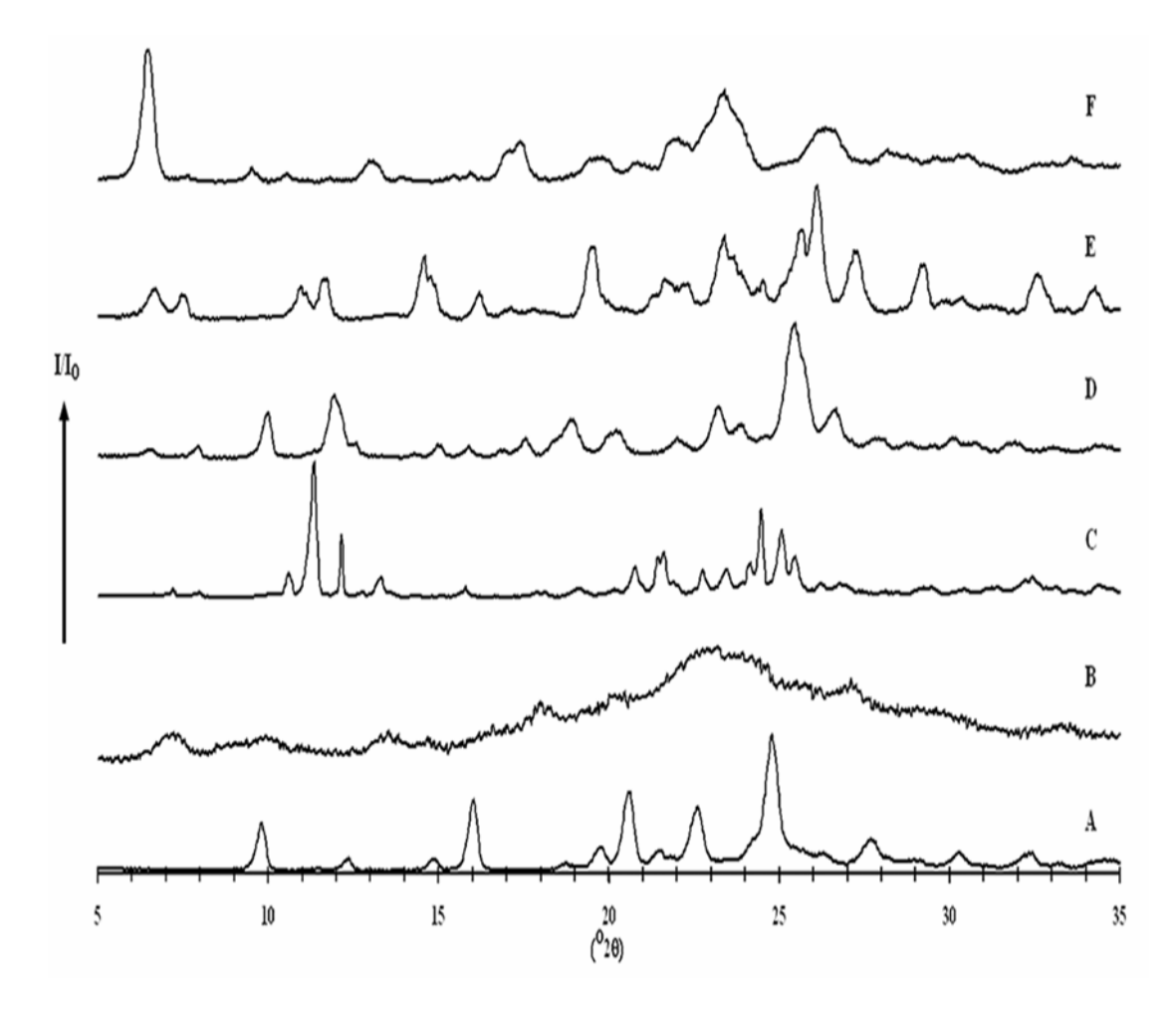


Figure 4 XRPD patterns of anhydrous NF Form A (A), disordered NF state (B), dihydrate NF (C), hemipentahydrate NF (D), trihydrate NF (E) and pentahydrate NF (F)

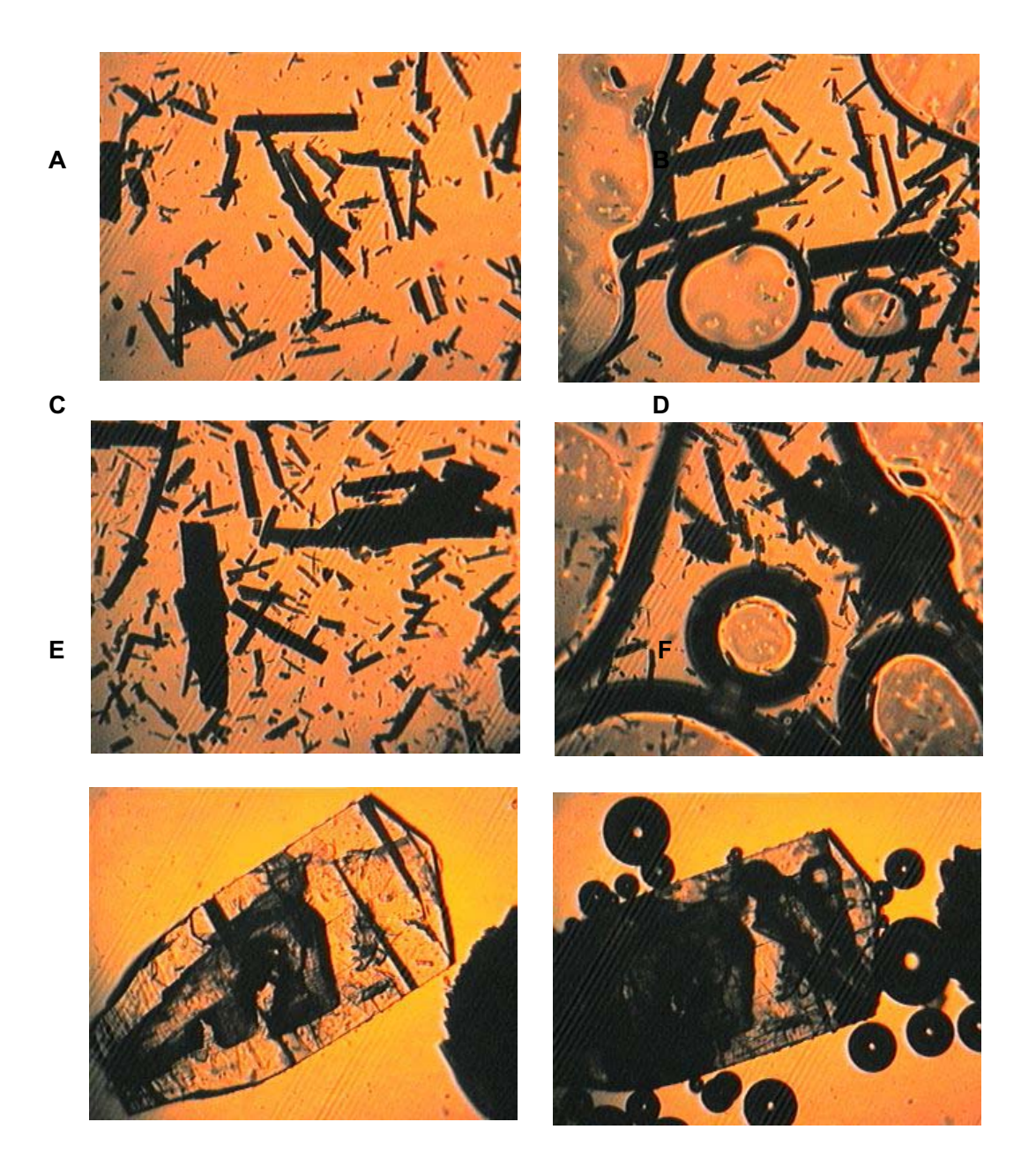


Figure 5 HSM photomicrographs of NF hydrates immerse in mineral oil upon heating (hemipentahydrate NF at ambient temperature (A), hemipentahydrate NF at temperarature over 120°C (B), pentahydrate NF at ambient temperature (C), pentahydrate NF at temperarature over 120°C (D), dihydrate NF at ambient temperature (E), dihydrate NF at temperarature over 100°C (F))

Pentahydrate NF, which was obtained from an alternative method of suspending anhydrous NF Form A in water also provided the same thermal behavior and XRPD pattern as the one hydrated NF at 100% RH. However, the crystal habits of the two pentahydrate NF were different. SEM micrographs of each solid were generated. Light yellow and coarse powder of anhydrous NF Form A (Figure 6A) was converted to opaque white, needle-like fluffy pentahydrate NF after having directly came into contact with water (Figure 6C). In contrast, exposure of anhydrous NF Form A to 100% RH did not change the appearance of the original powder (Figure 6A) even when the structure was found to be converted to the pentahydrate NF.

A different method of preparation and level of moisture in an environment greatly impacted on the formation of hydrate NF. The direct contact between anhydrous NF Form A with water was an issue. The precipitation of dispersed anhydrous NF Form A in excess amount of water was filtered and dried at ambient condition. An intact physical appearance of anhydrous NF Form A (light yellow fine powder) was rapidly converted to fluffy and waxy solid with opaque white color. SEM photomicrograph of solid obtained was fine needle-like particles fused together forming a network (Figure 6). It might be due to water partially dissolved the surface of anhydrous NF crystal and recrystallized and bridged together as NF hydrates. Light microscopy was used to investigate such phenomena. Anhydrous NF Form A with a drop of water was prepared on glass slide. The result suggested that the transformation of anhydrous NF Form A to the new unknown form immediately happened after contact with water (Figure 7B-D). The longer the contact time the more developed the new unknown NF form. The new unknown form was characterized and found to be pentahydrate NF. Thus, different methods of preparation could provide an identical internal structure of NF hydrate with different observable habit.

The phase transformation of anhydrous NF Form A to pentahydrate after direct contact with water is a valuable data for the pharmaceutical industries. Some made NF tablets by wet granulation with aqueous binder showed the physical transformation of powder blend after binder was added. The new physical character of the powder blend was hard and waxy agglomerates. It directly impact on the mixing efficiency and working capability of mixer. In the case of low efficiency mixer, mixer was usually broken during the mixing/granulating process. High efficiency mixer could overcome the above problem. However, the uniformity of powder blend was argued. It was suggested that a new phase in powder blend was strongly contributed from the transformation of anhydrous NF Form A to the pentahydrate NF with needle-like appearance. Non-aqueous binding solution was

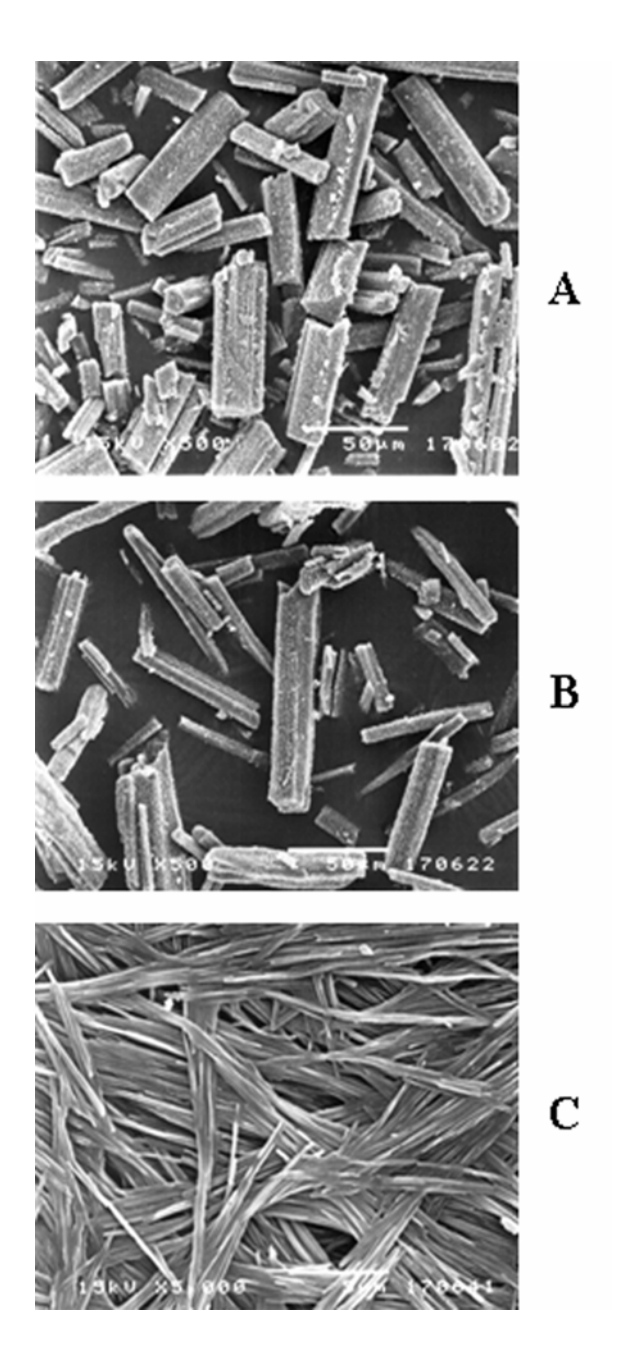


Figure 6 Scanning electron photomicrographs of anhydrous NF Form A (A), pentahydrate NF obtained from 100%RH vapor exposure (B) and pentahydrate NF from directly dispersed in water (C)

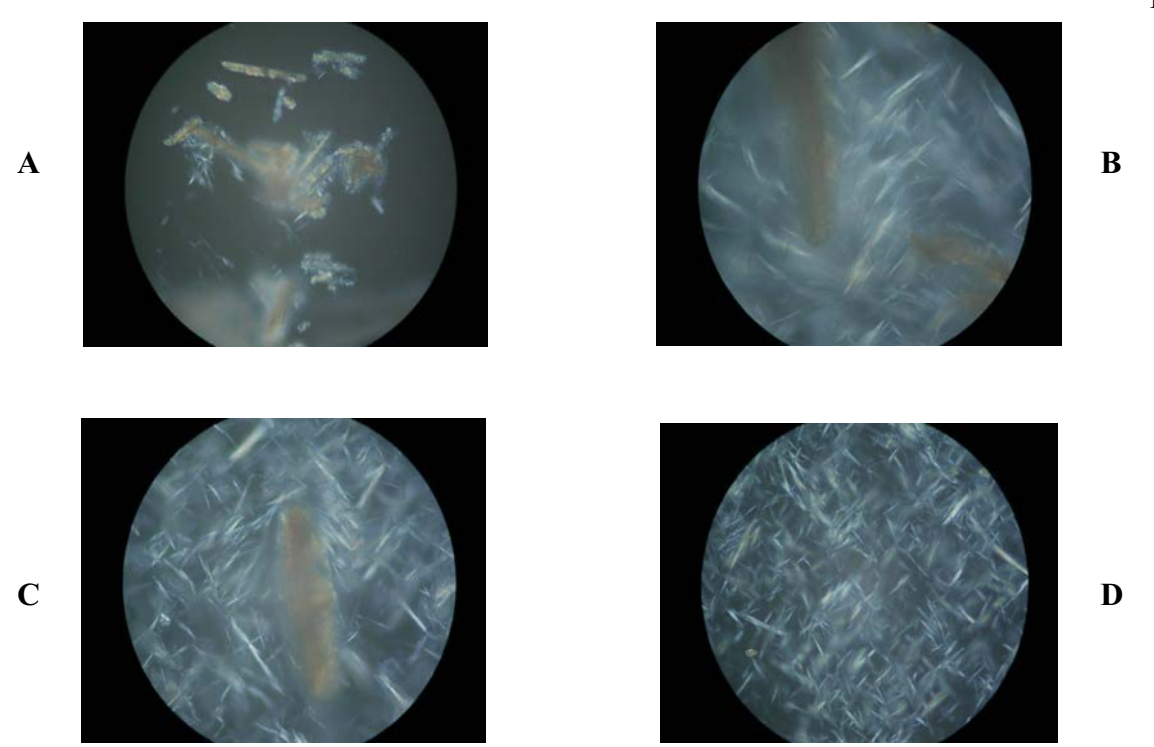


Figure 7 Photomicrographs of anhydrous NF Form A after dispersed in water at various contact time at the magnification of 400. (A. initial, B. 15 minutes, C. 60 minutes and D.180 minutes)

Another NF hydrate form found in this study, the disordered NF state, has not been previously reported elsewhere. Dehydration of pentahydrate NF via desiccation over time produced a so-called disordered NF state. DSC and TGA of the disordered NF state are shown in Figure 2B where a complex dehydration behavior was observed. Dehydration was detected during the first broad endotherm (100 °C) and immediately followed by a sharp exotherm (115 °C) and another broad endotherm. Mass loss of disordered NF state also took place over the same temperature range as found in the DSC. The sharp exotherm was possibly due to the rearrangement of NF molecules after water molecules were partially removed. Disordered NF provided an XRPD pattern similar to the amorphous material (Figure 4B). However, minor peak intensity in certain regions could still be observed. In comparison with amorphous NF (Šuštar et al., 1993), the DSC of disordered NF showed large endotherm with rapidly changing exotherm at the range of approximately 80 °C to 110 °C while amorphous NF exhibited an endotherm immediately followed by an exotherm from 80 to 150 °C. In addition, disordered NF showed two broad endothermic peaks while this thermal behavior was not seen in an amorphous NF upon heating. Thus, the disordered NF was believed not to be a true amorphous but only microcrystalline disorder state. The mild condition used to remove water molecules from pentahydrate NF might perturbed the crystal structure and led to a new arrangement or disordered state. Thus, short range order of crystal lattice was still preserved. Amorphous or disordered state generally occurred with anhydrous materials. However, some amorphous materials absorbed water molecules in the structure. For example, raffinose pentahydrate could become amorphous with water content equivalent to stoichiometric monohydrate (Hogan and Buckton, 2001).

In order to characterize the complex thermal behavior of the disordered NF, XRPD was utilized to monitor the molecular rearrangement of intact and heated disordered NF at predetermined times by using DSC. One sample was heated from 25 to 120 °C (D-I) and the other sample was heated from 25 to 160 °C (D-II). The DSC thermograms of heated sample of D-I and D-II are illustrated in Figure 8. DSC thermogram of D-I showed a complete disappearance of the initial complex thermal behavior comprised of large endotherm with followed by rapid exotherm. Subsequently, D-II exhibited the thermogram consisted of only second endotherm after the initial thermal event was removed. It indicated that two complex thermal events of disordered NF did not have any interaction together. After the first two events were removed, DSC thermogram displayed only one sharp endotherm correlated to the melting endotherm of anhydrous NF Form A. It could be initially concluded that two locations of water molecules of disordered NF were separated in different lattice space. Moreover, the XRPD pattern of D-I is displayed in Figure 9B. It showed increased in crystallinity compared to the initial disordered NF. Initial disordered NF was also heated from and its XRPD pattern is illustrated in Figure 9C. The solid obtained after D-II exhibited higher order than that of initial disordered NF and after D-I treatment. The XRPD pattern was shown to be identical to that of the anhydrous NF Form A. TGA confirmed that the solid obtained after D-II treatment showed no weight loss. It could, hence, be concluded that solid collected after D-II treatment is an anhydrous Form A. The total weight change from D-I to D-II was approximately 1.64% which was higher than the value allowed for anhydrous NF in the official monographs (less than 1%) (USP 27; BP 2002). Thus, the solid resulted from D-I treatment was a hydrated transitional phase which, in turn, would convert to the anhydrous Form A upon further heating. In addition, the water content of hydrated transitional phase obtained from TGA was in the range of 2.5 to 3.5 %w/w that was in the range of hemipentahydrate NF form. It should be indicated the hydrated transitional phase was the one hydrate form of NF.



STAR® SW 8.01

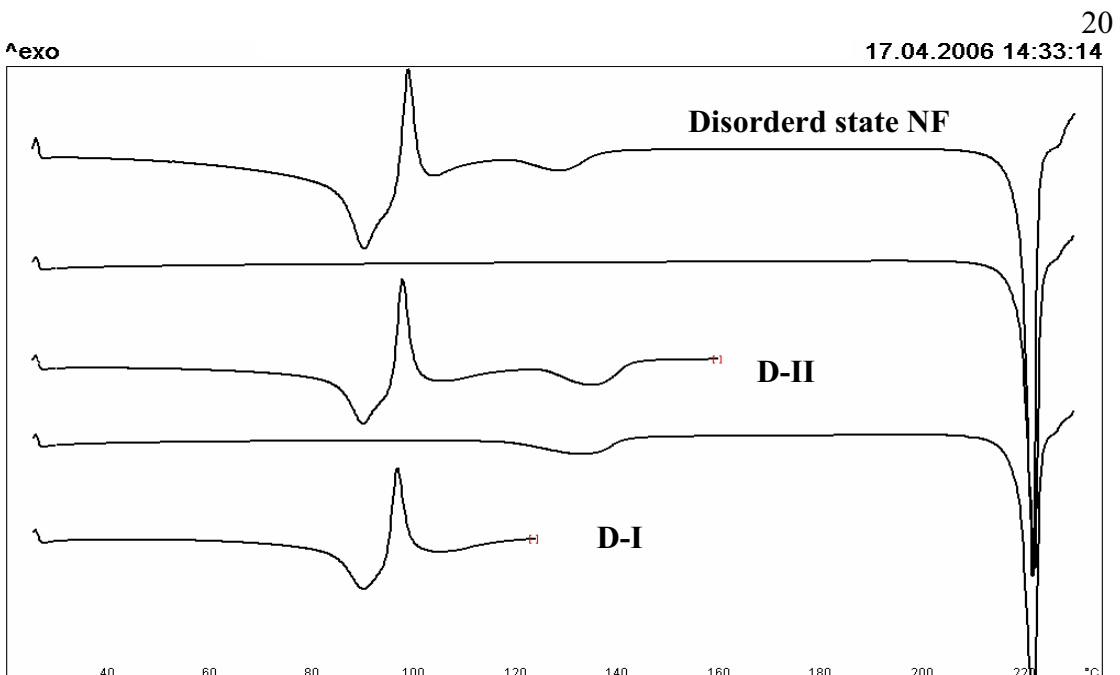
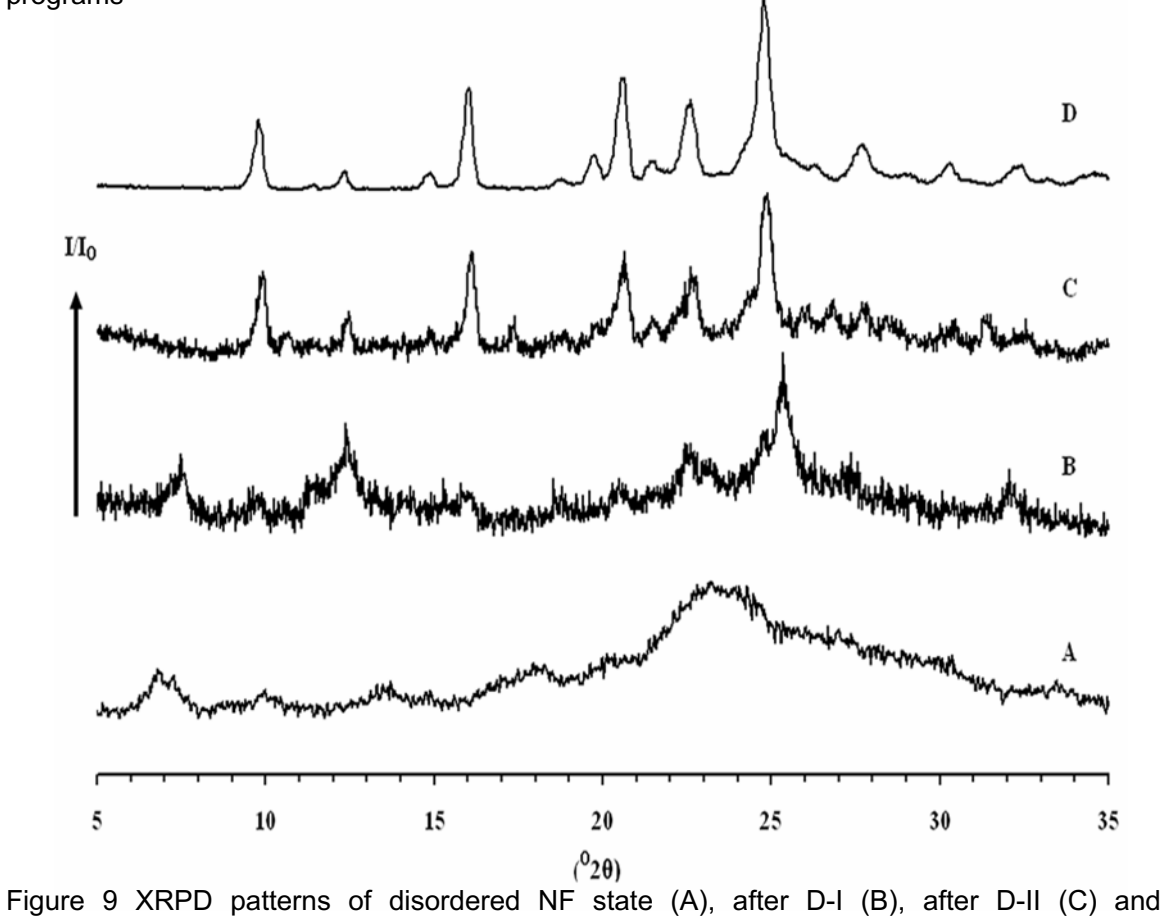


Figure 8 DSC thermograms of disordered NF with respect to different heating temperature programs

Lab: METTLER



anhydrous NF Form A (D)

In general, materials of disordered molecular arrangement are more sensitive to moisture than the ordered crystalline phase. Consequently, the moisture sensitivity of the disordered NF was a critical issue. The disordered NF was thus exposed to various humidity levels for 7 days and the XRPD patterns were recorded (Figure 10). The transformation of the disordered NF to the crystalline pentahydrate NF form was completed when at least 57% RH was used. At 32.8% RH, partial transformation to the pentahydrate was seen according to the presence of peaks at 6.40, 13.00, 17.28, 23.36 and 26.20 °2 $\theta$ . On the other hand, the disordered NF state was stable under 11.3% RH for at least 2 months similar to the XRPD pattern after 7 days exposure to 11.3% RH. Thus, exposing the disordered NF to more than 32.8% RH would eventually generate the crystalline pentahydrate NF. However, at humidity of 11.3% RH or below, the disordered NF structure was retained.

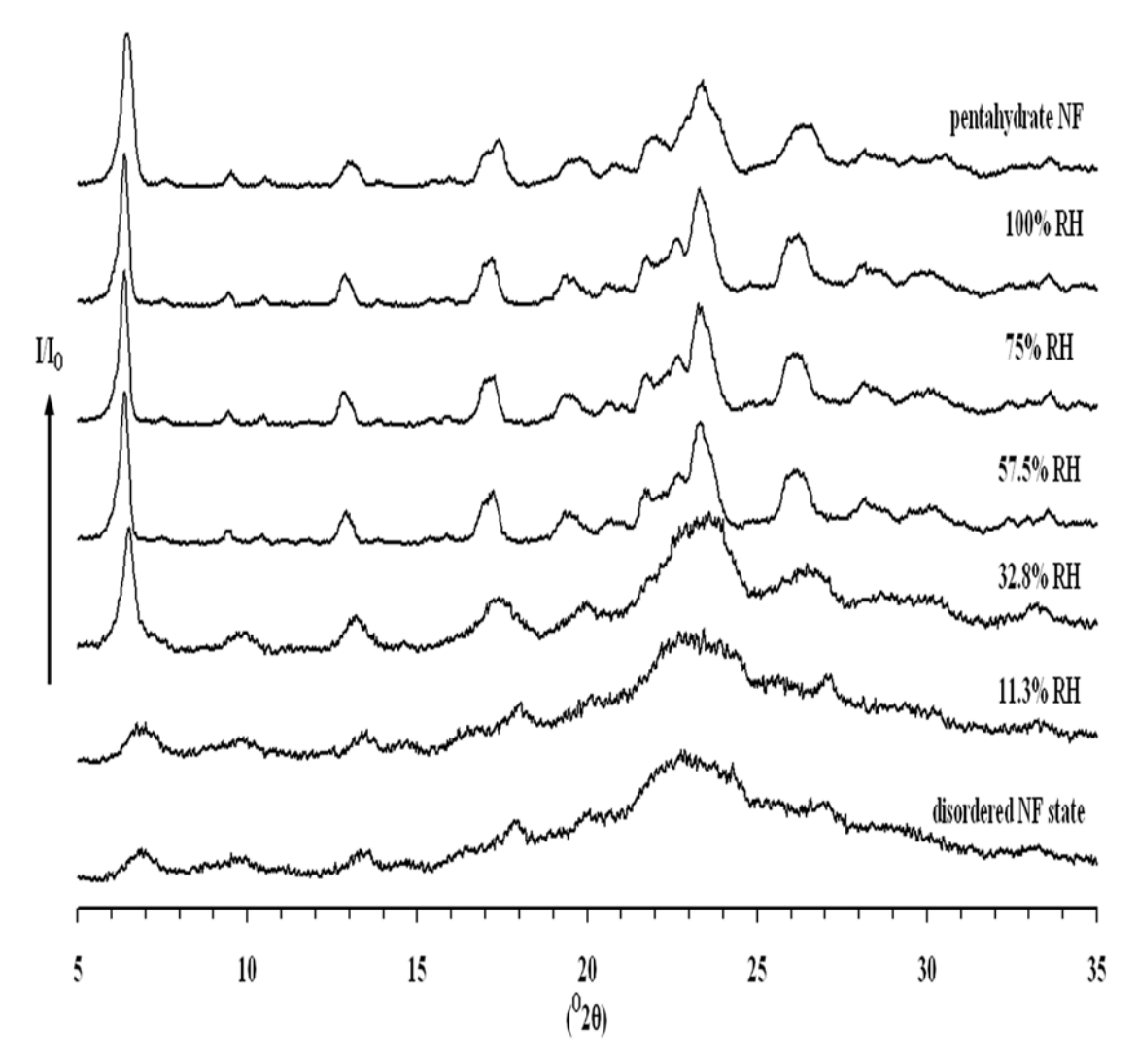


Figure 10 XRPD patterns of disordered NF states exposed to different relative humidity for 7 days

Chemical interaction between water of crystallization and active moiety of every NF hydrate was investigated by spectroscopic FT-IR. The spectra of every NF hydrate form were recorded and compared (Figure 11). The signal at specific wavenumber can be interpreted in terms of the functional group of the material. The IR spectrum of anhydrous NF Form A exhibited main absorption peaks at 1732 and 1253 cm<sup>-1</sup> indicating C=O and C-O bond stretching of carboxylic group, respectively. When water molecules are incorporated into the crystal structure, the response of C=O and C-O are found to gradually decrease as a function of increased number of water of crystallization (Mazuel, 1991). Meanwhile, the responses at 1584 and 1340 cm<sup>-1</sup> of carboxylate anion are markedly increased. The above results suggested that structures of the carboxylic group in these hydrates are the carboxylate anion (Hu et al., 2002). In addition, the responses in the regions of 3700 to 3250 cm<sup>-1</sup> owing to OH stretching were clearly present in all NF hydrates, signifying hydrogen bonding between carboxylic group and water molecules in the crystal structure (Byrn et al., 1999). The FT-IR spectrum of the disordered NF was also investigated. The presence of peaks at 1581 and 1334 cm<sup>-1</sup> confirmed the occurrence of carboxylate anion identical to other hydrates and the lack of responses at 1732 and 1253 cm confirmed that C=O and C-O stretching of carboxylic group was disturbed by water molecule as well. It can be concluded that water molecules in disordered NF formed structural hydrogen bonds with NF molecules similar to those of other stoichiometric hydrates. Thus, it is believed that the disordered NF form was not a true amorphous state but a metastable phase with short range ordered structure.

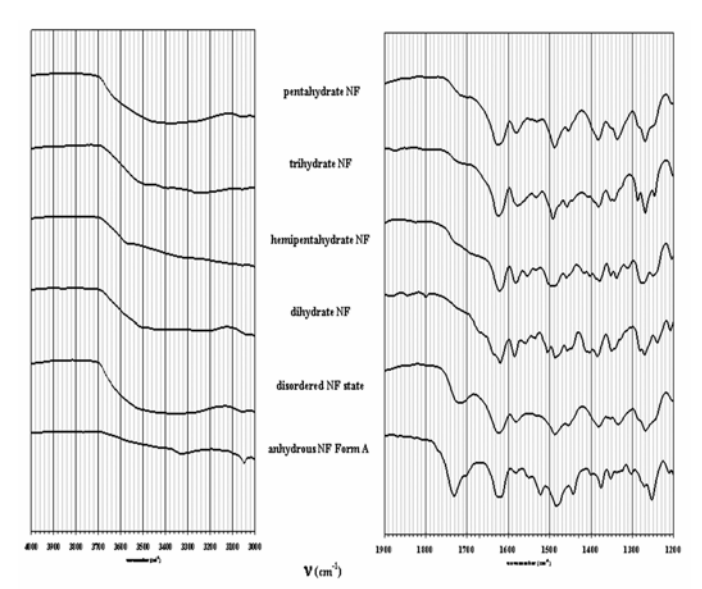


Figure 11 FT-IR spectra of anhydrous NF Form A, disordered NF state and other stoichiometric hydrates of NF

#### **Solid State Interconversion of NF Hydrates**

XRPD patterns of NF hydrates (Figure 4) were used as reference patterns to show specific characteristics of each form and were used to identify the solid state transformation. The following studies gathered evidences on the solid state transformation of NF hydrates under different environmental i.e. relative humidity and temperature. It should be noted that the observed trends are based on visual inspection of the diffraction patterns and are not intended to be quantitative.

#### Effect of Relative Humidity on Solid State Transformation of NF Hydrates

Moisture content in the environment usually plays the most pivotal part in hydrate formation of many organic compounds (Zhu et al., 1996a; Zhu and Grant, 1996b). The anhydrous NF Form A placed under different %RH were found to form varying stoichiometric NF hydrates (Katdare et al., 1986; Yuasa et al., 1982). The moisture sorption study was used as a rough evaluation on the hydrate formation behavior due to moisture. Moisture vapor sorption data of the anhydrous NF Form A obtained by DVS showed that under 60% RH, the anhydrous structure was retained (Figure 12). On the other hand, at moisture levels higher than 60% RH, anhydrous NF Form A showed a marked mass increase. The higher the relative humidity of the environment above 60% RH the higher the weight gain. The final solid structure formed at the end of the sorption phase was later found to be the pentahydrate NF by XRPD.

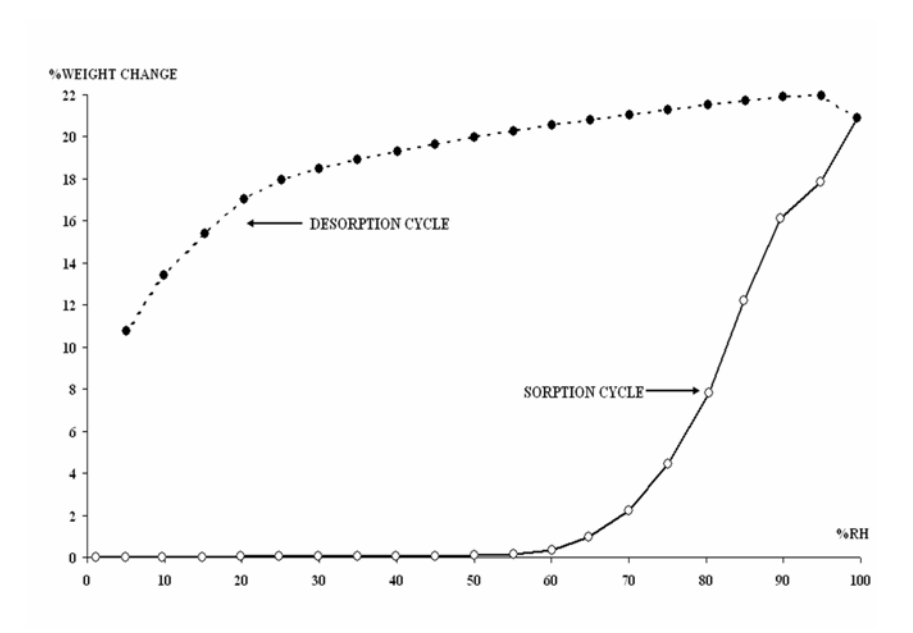


Figure 12 Dynamic water vapor moisture sorption and desorption isotherms of anhydrous NF Form A at 25°C

Desorption phase of the induced the pentahydrate NF showed that the pentahydrate NF was very stable even at below 30% RH. However, when the environment reached very low humidity of below 20% RH, significant weight loss occurred. The result suggested that for dehydration of the pentahydrate NF to occur the environment must reach very low relative humidity. These data could be used to determine a suitable storage condition of NF raw material. The suggested storage condition for the anhydrous NF Form A should be in an environment where moisture level is not more than 60% RH at room temperature. The pentahydrate NF form should not be stored in areas where relative humidity is below 20% RH to prevent dehydration.

The degree of hydration of anhydrous NF Form A with respect to relative humidity was investigated and characterized by XRPD (Figure 13). The hemipentahydrate NF was achieved when anhydrous NF Form A was exposed to 75%RH as mentioned in the previous section. XRPD patterns of the anhydrous NF Form A which were stored between 81%RH to 87%RH, however, showed mixed characteristics at 6.48 °2 $\theta$  and 25.48 °2 $\theta$  of the pentahydrate NF and the hemipentahydrate NF, respectively. Increasing the moisture level was found to accentuate the intensity of the peak at 6.48 °2 $\theta$ . Meanwhile the intensity at 25.48 °2 $\theta$  was reduced. When anhydrous NF Form A was exposed to humidity higher than 93.7%RH, pure pentahydrate NF was found. In addition, exposure of the anhydrous NF Form A at very high humidity did not generate any degradation products as confirmed by SI-HPLC.

NF hydrates were placed under 100%RH for 7 days after which XRPD patterns were recorded. The XRPD results revealed that every sample converted to the pentahydrate NF, except the dihydrate NF. The dihydrate NF exposed to 100% RH showed mixed characteristics of both dihydrate NF and pentahydrate NF (Figure 14). It could be inferred that the pentahydrate NF was the most stable form in extremely high moisture environments.

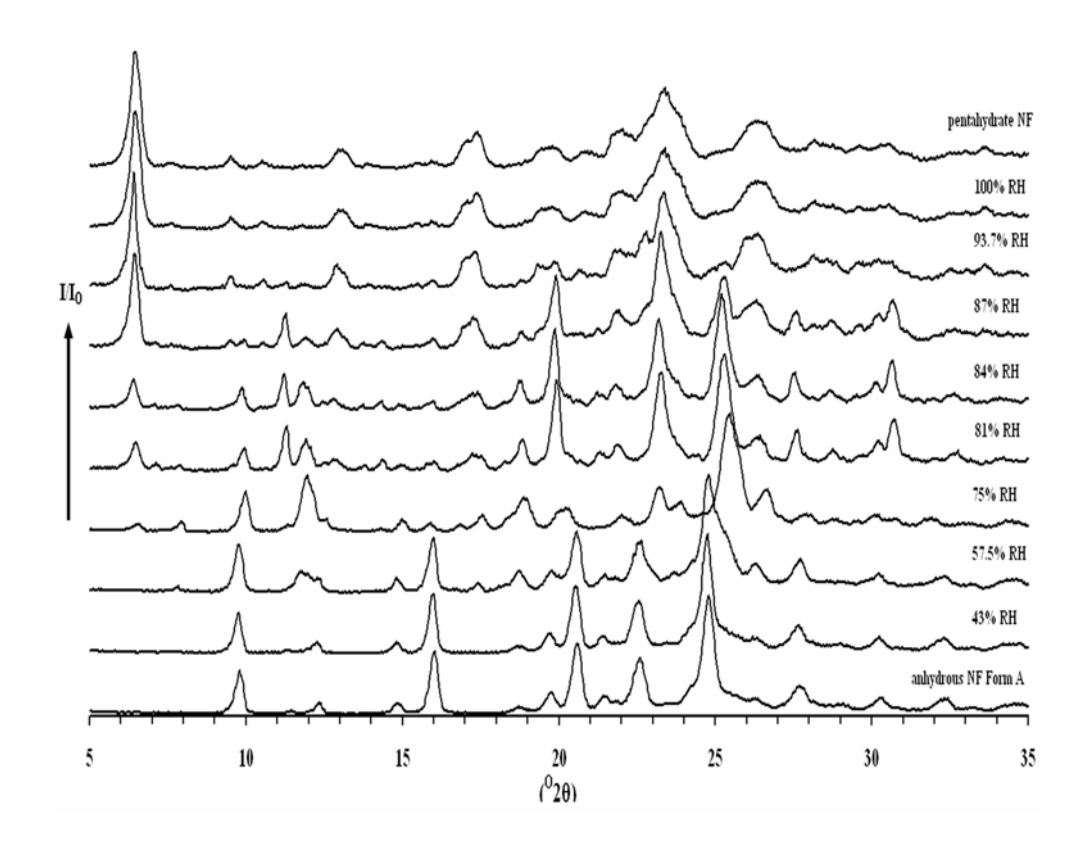


Figure 13 XRPD patterns of anhydrous NF Form A under different relative humidity for 7 days

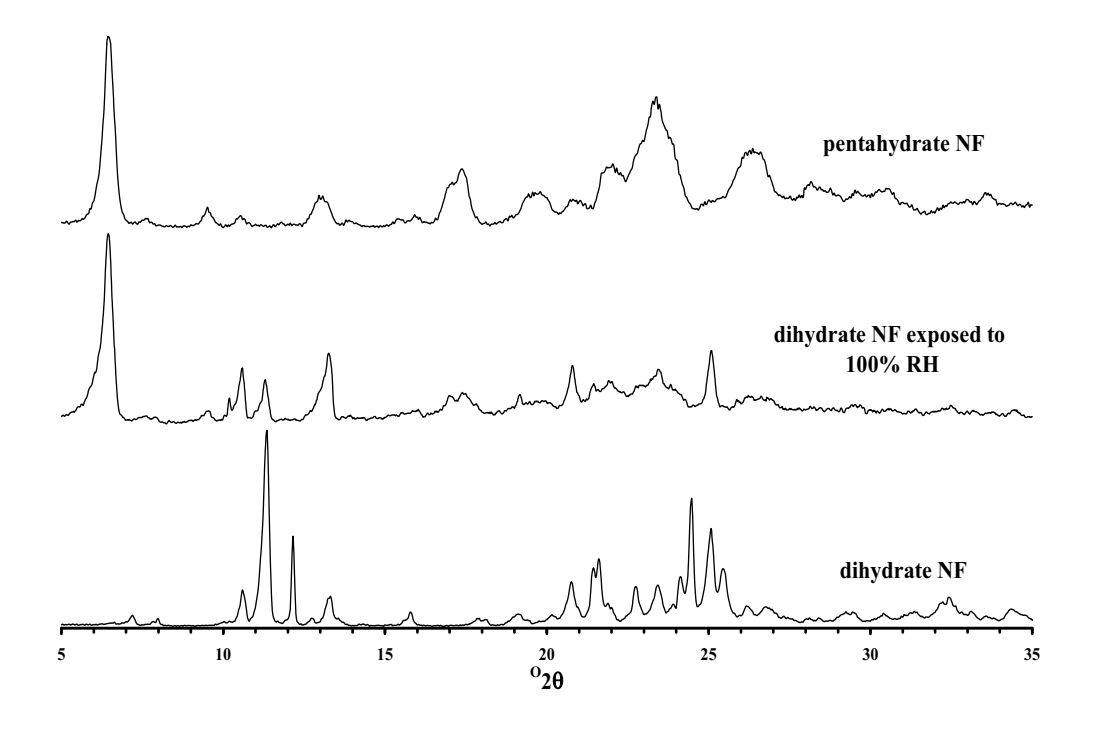


Figure 14 XRPD patterns of dihydrate NF under 100% RH for 7 days

On the other hand, the reduction to near 0%RH was also investigated. The pentahydrate NF was transformed to the disordered NF state as discussed earlier. The XRPD pattern of the hemipentahydrate NF at 0% RH is illustrated in Figure 15. The characteristic peak at 25.48 °2 $\theta$  was slightly shifted to lower angle of 24.84 °2 $\theta$  which corresponded to the anhydrous NF Form A. Meanwhile, the intensity at 26.68 °2 $\theta$  gradually decreased as a function of exposure time. The longer contact time to dry environment led to the formation of a mixture of the two forms. The trihydrate NF showed the same phenomenon on the conversion to the anhydrous NF Form A during exposure to 0% RH condition. The XRPD patterns of the trihydrate NF during dehydration are shown in Figure 16. After 7 days of dehydration, peak responses at 9.84, 20.52 and 24.84 °2 $\theta$  of the sample were found to be of the anhydrous NF Form A. Peak positions at 7.52 and 25.40 °2 $\theta$  were also apparent and related to the hydrated transitional phase similar to the heat treated (D-I) of the disordered NF state (Figure 9B). Meanwhile, other strong and characteristic trihydrate peaks still existed. In summary, dehydration by reduction of effective environmental moisture was not an method to convert neither the hemipentahydrate NF nor the trihydrate NF to the pure anhydrous NF Form A even after 90 days exposure. Therefore, the dihydrate NF was not further evaluated due to lack of dehydration efficiency by this approach.

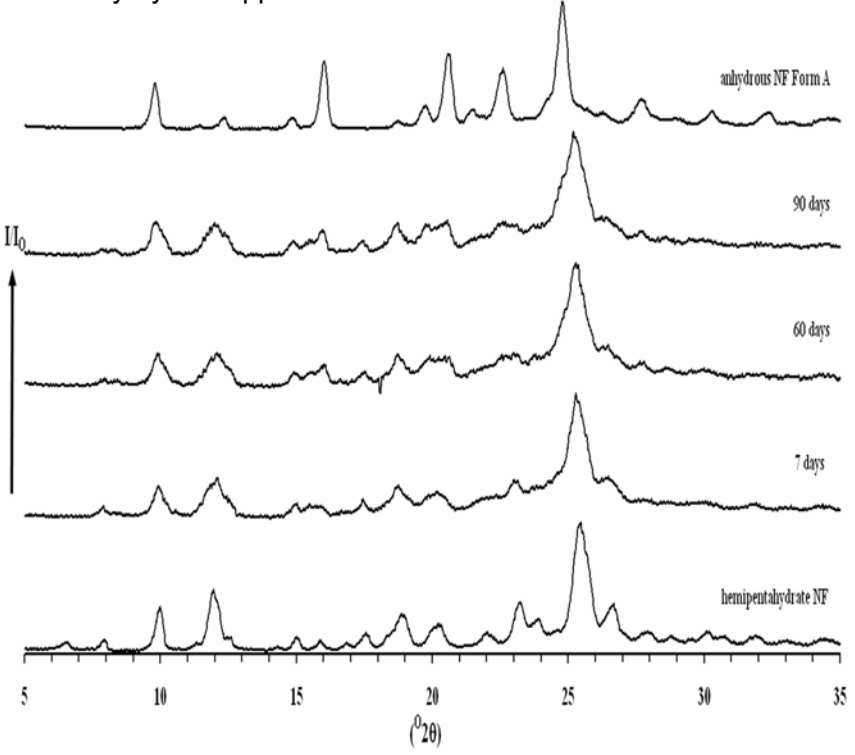


Figure 15 XRPD patterns of hemipentahydrate NF under desiccant (0% RH) as a function of exposure time

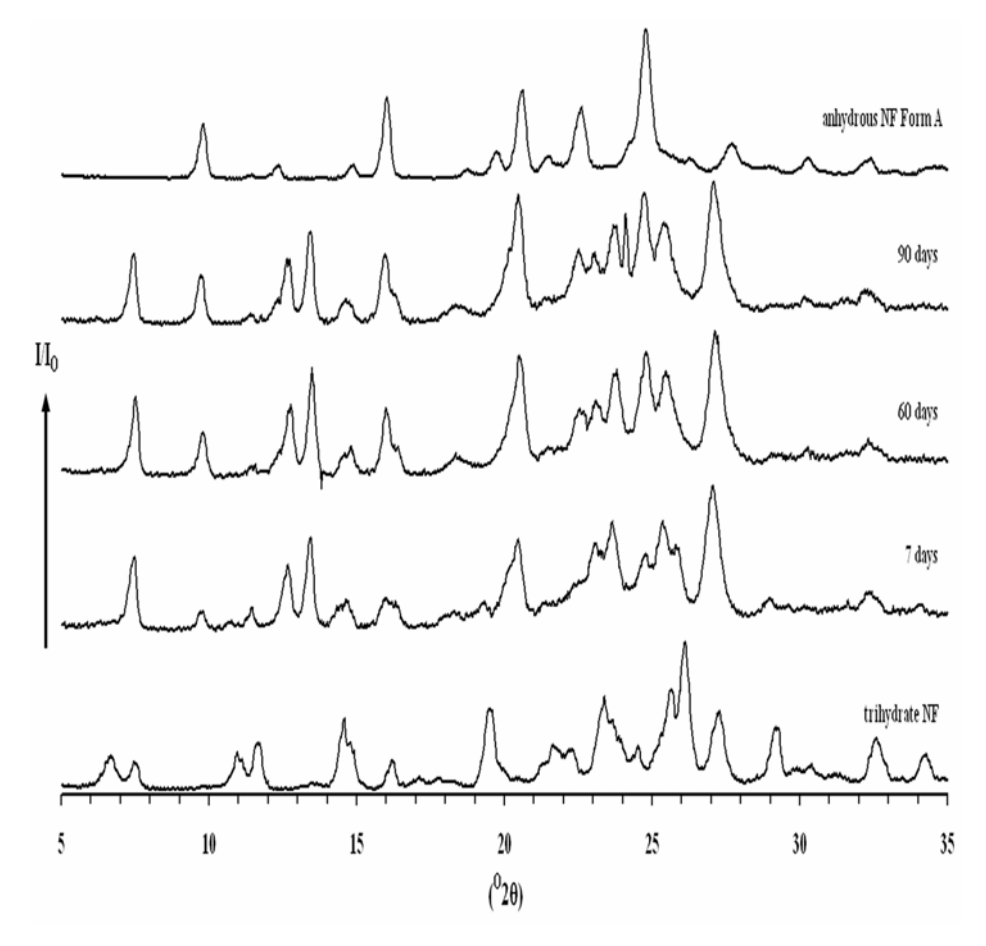


Figure 16 XRPD patterns of trihydrate NF under desiccant (0% RH) as a function of exposure time

## Effect of Elevated Temperature on Solid State Transformation of NF Hydrates

Thermal dehydration is the most common way to prepare anhydrous materials in the pharmaceutical industry. There are many publications reported the polymorphic transformation or occurrence of desolvation upon thermal treatment (Lin and Chien, 2003; Willart et al., 2002; Landgraf et al., 1998; Hakanen and Laine, 1995). Hence, the conversion of NF hydrates using selected elevated temperature was performed. In this study, a moderate temperature of 60 °C was selected to minimize potential chemical degradation associated with higher temperatures.

The disordered NF was heated at 60 °C for 48 hours. XRPD showed that the anhydrous NF Form A was transformed from the disordered NF after heating (Figure 17B). The residual water content of the heated samples was investigated using KF. The water contents were 1.02, 0.60 and 0.46 for heated samples of the disordered NF, the hemipentahydrate NF and the pentahydrate NF, respectively. The results revealed that all heated samples were essentially anhydrous because the water content was approximately

at or below the maximum limit (1%) for NF anhydrous specified in the monograph (USP 27; BP 2002). In the case of the heated hemipentahydrate NF, the XRPD pattern was similar to that of the disordered NF (Figure 17C). Note that the heated pentahydrate NF resulted in a similar XRPD pattern to that of the anhydrous Form A but with two additional peaks at 7.52 and 25.40 °2 $\theta$  (Figure 17D). These two peaks were assumed to be the residual of the hydrated transitional phase (Figure 9B) found during D-I treatment of the disordered NF state.

The results from the heated dihydrate NF and the heated trihydrate NF are shown in Figures 18 and 19, respectively. The XRPD of the dehydrated dihydrate NF revealed that a partial anhydrous phase was generated after thermal dehydration for 48 hours. However, peaks at 10.60, 11.32 and 13.16 and 25.00 °2 $\theta$  corresponding to the dihydrate NF were still present. Extended heating time of up to 1 month gave material with an identical pattern to that of the 48-hour treated sample. Thus, the longer heating time did not fully convert the dihydrate NF to the anhydrous NF Form A. The trihydrate NF also behaved in the same way upon thermal dehydration. XRPD of the treated trihydrate NF showed the anhydrous Form A peaks at 9.80, 16.04, 22.68 and 24.84 °2 $\theta$ . Additional peak position at 7.52 and 25.40 °2 $\theta$  were also noticeable and related to the hydrated transitional phase while the trihydrate NF peak at 23.36 °2 $\theta$  remained pronounced indicating a mixture of the three forms. Extended thermal dehydration of the trihydrate NF at 60°C of up to 1 month did not generate the pure anhydrous NF Form A.

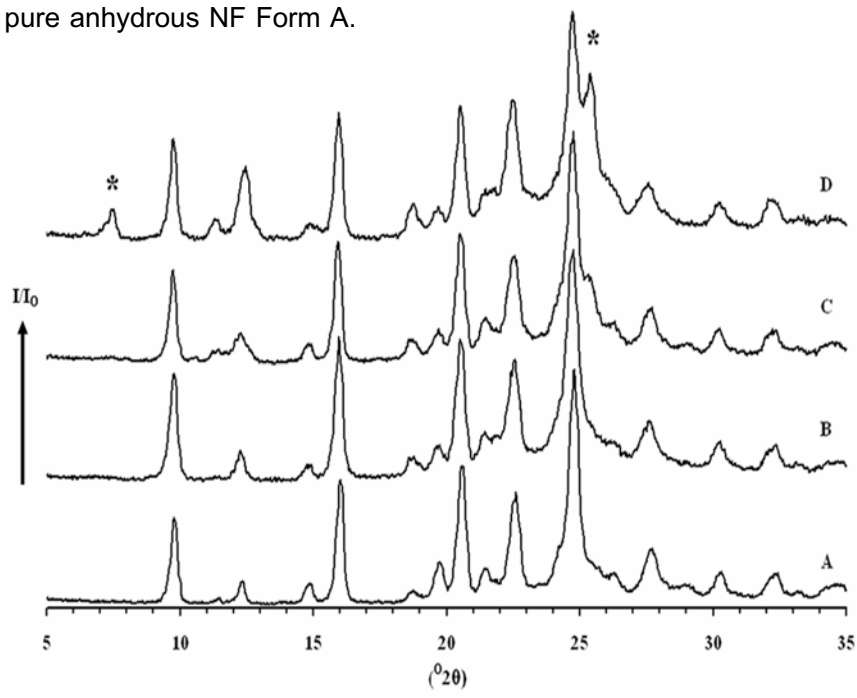


Figure 17 XRPD patterns of anhydrous NF Form A (A), disordered state NF (B), hemipentahydrate NF (C) and pentahydrate NF (D) after heated at 60°C for 48 hours

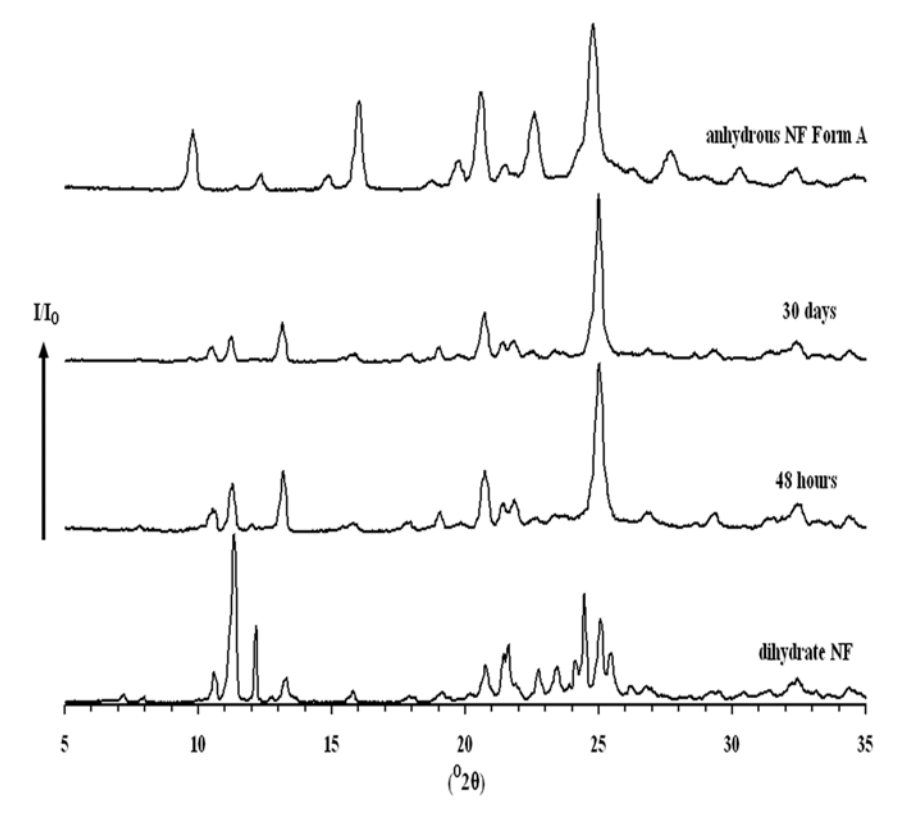


Figure 18 XRPD patterns of dihydrate NF after heated at 60°C for various time period

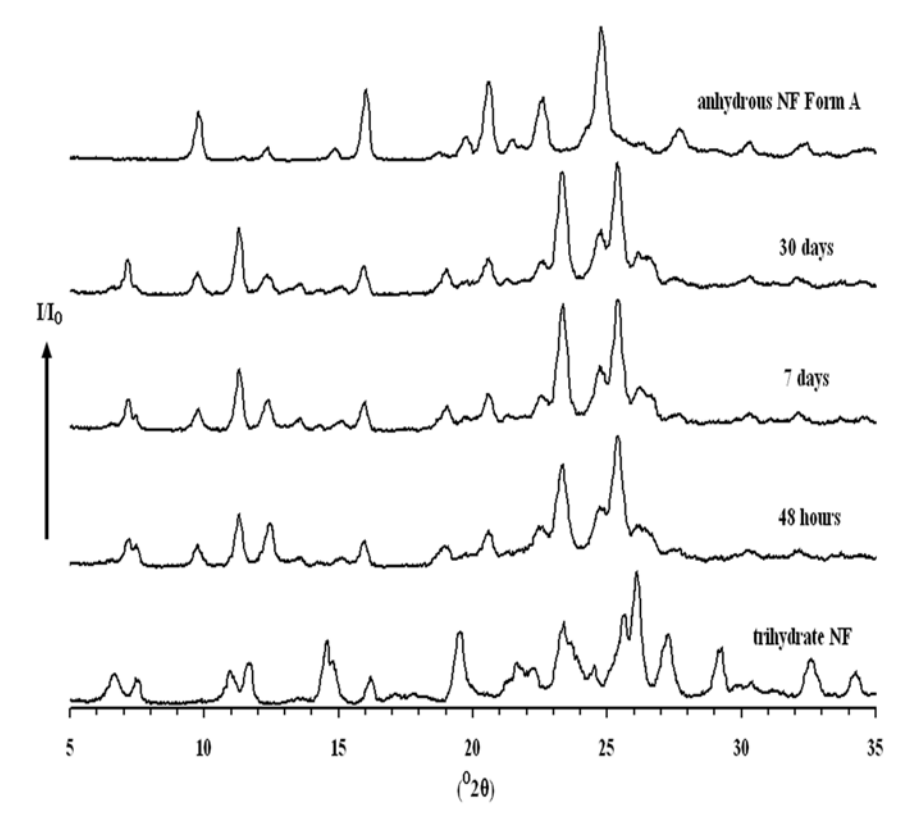


Figure 19 XRPD patterns of trihydrate NF after heated at 60°C for various time period

The solid state interconversion of NF hydrates is summarized in Figure 20. The anhydrous NF Form A and the other hydrate forms transformed to the pentahydrate NF when exposed to saturated water vapor. Meanwhile, the anhydrous NF Form A could be produced from thermal dehydration of the disordered NF state and hemipentahydrate NF. On the contrary, dihydrate NF, trihydrate NF and pentahydrate NF were not fully converted to the anhydrous NF Form A upon heating. Dehydration of NF hydrates with the aid of desiccant did not provide pure anhydrous NF Form A. Instead, it generated the disordered NF state from the pentahydrate NF. The disordered NF state had specific rehydration behavior and instability against humidity such that it could easily be transformed to the pentahydrate NF starting at very low moisture of 32.8% RH compared to the anhydrous NF Form A where it needs 93.7% RH to convert to the pentahydrate NF.

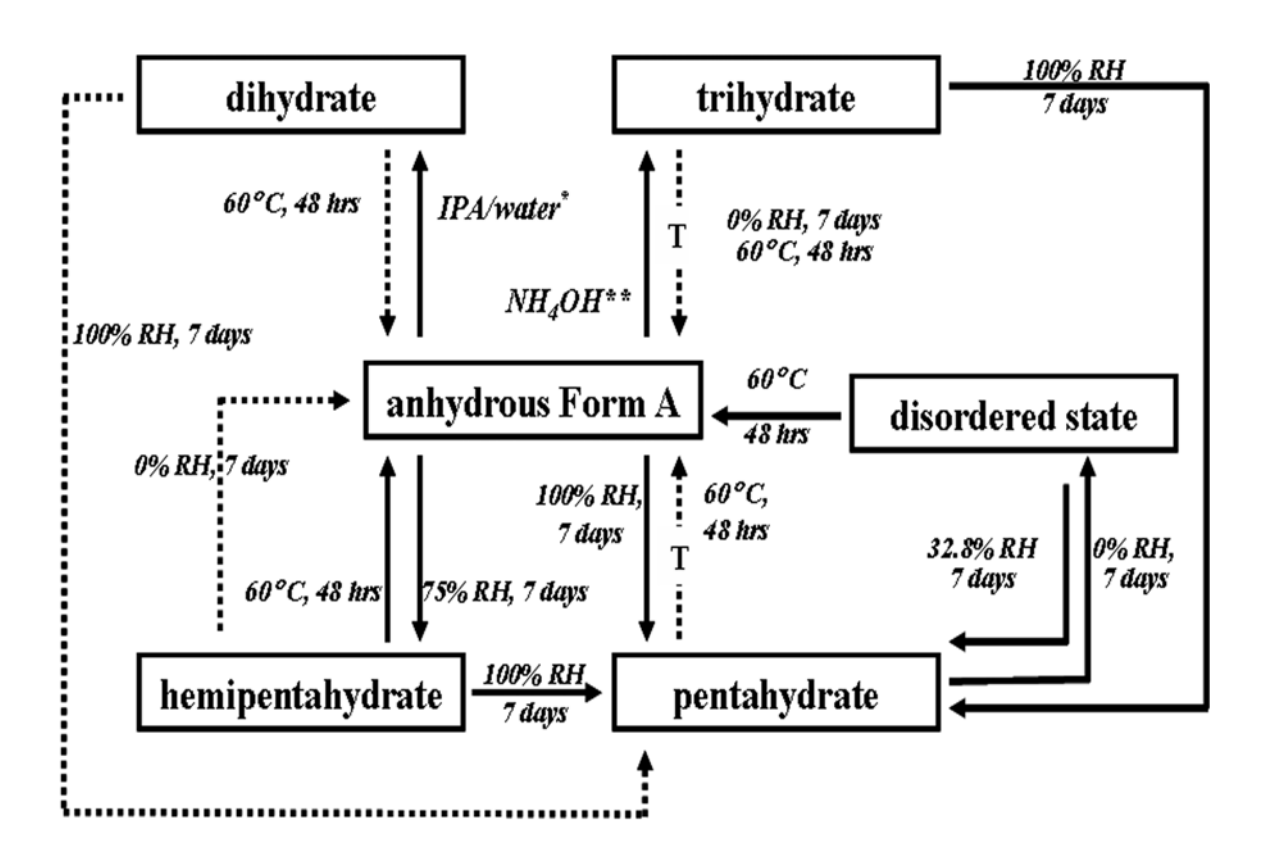


Figure 20 Summary of the solid state interconversion of anhydrous NF Form A and its hydrates ( = complete transformation, --- = incomplete transformation, T = hydrated transitional phase or hemipentahydrate NF, \* = the dihydrate NF derived from recrystallization in the mixture of IPA and water, \*\* = the trihydrate NF generated by antisolvent precipitation from aqueous ammonia NF solution)

## Isothermal Dehydration of Hemipentahydrate NF

IDSC patterns during dehydration of hemipentahydrate NF are illustrated in Figure 21. The  $T_{iso}$  of hemipentahydrate NF at various  $T_{iso}$  were different and depend on the nature of dehydration. The  $T_{iso}$  was determined by observing an unchanged power in IDSC thermograms. The  $T_{iso}$  of the dehydration of hemipentahydrate NF was determined to be at 180 mins at 95  $^{\circ}$ C and 300 mins at 80  $^{\circ}$ C, 85  $^{\circ}$ C and 90  $^{\circ}$ C. IDSC patterns of all hemipentahydrate NF showed two steps consecutive dehydration. However, the dehydration steps were not clearly separated. Energy calculation of the dehydration process was possible only when dehydration was completed. The AUC of IDSC patterns at various  $T_{iso}$  were calculated and are tabulated in Table 2. The result revealed that dehydration energies at every  $T_{iso}$  were insignificantly different. It could be concluded that the total energy needed for dehydration of hemipentahydrate NF was temperature independent within the investigated range of 80  $^{\circ}$ C to 95  $^{\circ}$ C.

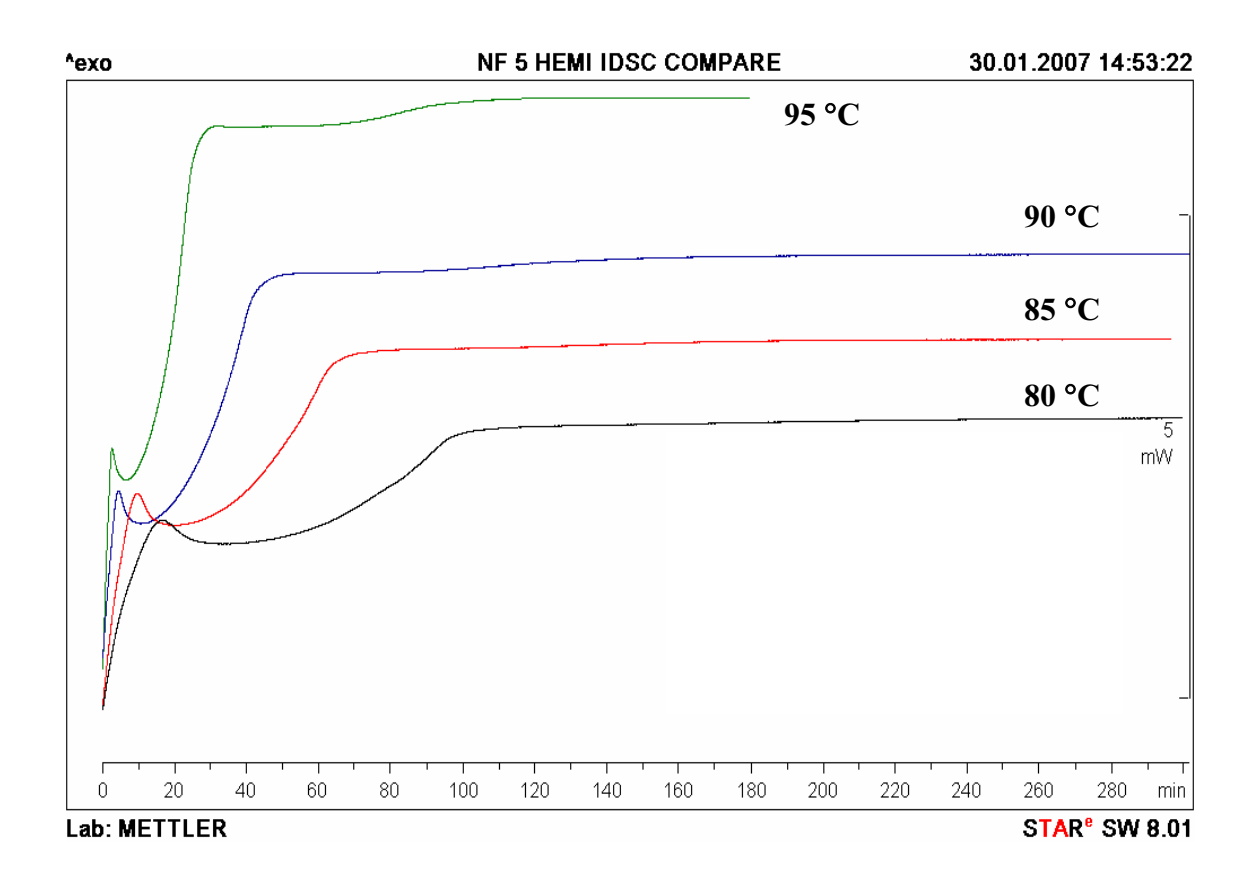


Figure 21 IDSC thermograms of hemipentahydrate NF during isothermal dehydration at various  $T_{\rm iso}$ 

Table 2 Dehydration energy, residual water content and particle size of dehydrated hemipentahydrate NF after complete dehydration at different  $T_{\rm iso}$ 

T <sub>iso</sub> (°C)	Dehydration energy	Residual water content	d [v,0.5]
	(J/g)	by TGA (%w/w)	(micron)
Intact form	-	12.12 ± 0.04	248.88 ± 2.91
80	285.12 ± 5.34	$0.38 \pm 0.06$	240.68 ± 5.53
85	290.33 ± 6.57	$0.43 \pm 0.36$	225.03 ± 8.16
90	292.38 ± 5.75	0.37 ± 0.27	212.17 ± 5.89
95	277.57 ± 12.56	0.24 ± 0.13	237.13 ± 1.50

The residual water contents of all dehydrated hemipentahydrate NF were lower than 1% w/w (Table 2) indicating the generation of the anhydrous phase of NF. XRPD of every dehydrated hemipentahydrate NF after exposure to different  $T_{iso}$  showed the specific character of anhydrous NF Form A (Figure 22).

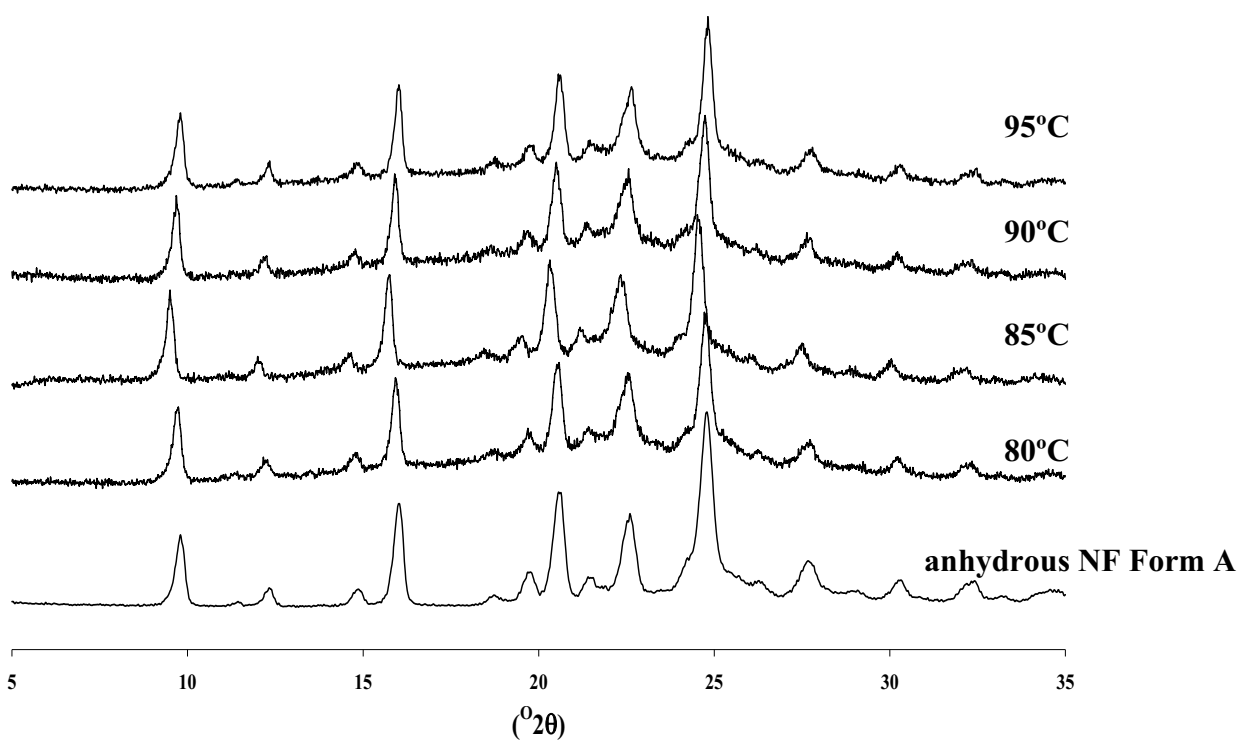


Figure 22 XRPD diffractograms of dehydrated hemipentahydrate NF after isothermal dehydration with respect to  $\mathsf{T}_{\mathsf{iso}}$ 

Investigation of particle size changes during dehydration are also demonstrated in Table 2. According to statistical comparison, the difference of particle size between intact hemipentahydrate NF and all dehydrated hemipentahydrate NF were found to be significantly different (p<0.05). The particle sizes of intact hemipentahydrate NF and dehydrated samples at 85 °C and 90 °C were significantly different (p<0.05), while there was no difference between the particle size of intact hemipentahydrate NF and the dehydrated samples at 80 °C and 95 °C. It might be due to the fact that the particle size reduction of hemipentahydrate NF depends on the heating rate at different  $T_{\rm iso}$  while dehydration energies of all dehydrated samples were similar. At the lowest T<sub>iso</sub> of 80 °C, SEM photomicrographs did not show particle size disruption (Figure 24). SEM photomicrographs of dehydrated hemipentahydrate NF at higher  $T_{iso}$  of 85  $^{\circ}C$  and 90  $^{\circ}C$ showed surface defects and resulted in the smaller particles of anhydrous NF Form A. However, at the highest T<sub>iso</sub> of 95 °C, anhydrous barrier was rapidly generated and retard the escape of water molecules and led to the retained hydrated structure. The statistically significant difference in particle size between intact and dehydrated hemipentahydrate NF was determined but it could not be concluded that the particle size reduction was evident because the maximum difference was within the range of 25 micron. Thus, the apparent energy used for particle size reduction of hemipentahydrate NF by isothermal dehydration was not determined in this study.

The relationship between fraction reacted  $(\alpha)$  and time (t) of dehydration of hemipentahydrate NF by model dependent solid state kinetic are presented in Figure 23. It was directly derived from IDSC data at each  $T_{iso}$  and showed two steps of dehydration from observable two phases of the slopes. The calculated  $E_a$  with different solid state kinetic equations were in the range of approximately 76 kJ/mol and 120 kJ/mol for the early and the later stage of dehydration, respectively. The Avrami Eroféev equations with one and two dimensional gave a good fit of the dehydration of hemipentahydrate NF. The random nuclei generated along one or two dimensions and progressively ingested other nuclei was defined as main mechanism of dehydration. Beside, the phase boundaries model also showed good agreement. It indicated the advancement of dehydrated phase from the outside of particle concerned to the inside. Therefore, the main mechanism of dehydration was not able to be explained by either single Avrami Eroféev model or Phase Boundaries model. Model independent approach resulted in  $E_a$  in between of 80 to 120 kJ/mol which was similar to the  $E_a$  obtained from model dependent (Figure 25). These results indicated that the "rate" of dehydration of hemipentahydrate NF for both steps depended on the

dehydration temperature. The higher  $E_a$  of the initial step of dehydration strongly indicated the temperature dependency of the dehydration rate. On the other hand, the gradual and continuous decrease in  $E_a$  during dehydration indicated less energy barrier for dehydration which resulted from the disruption of the structural integrity of hydrate particles without particle size reduction.

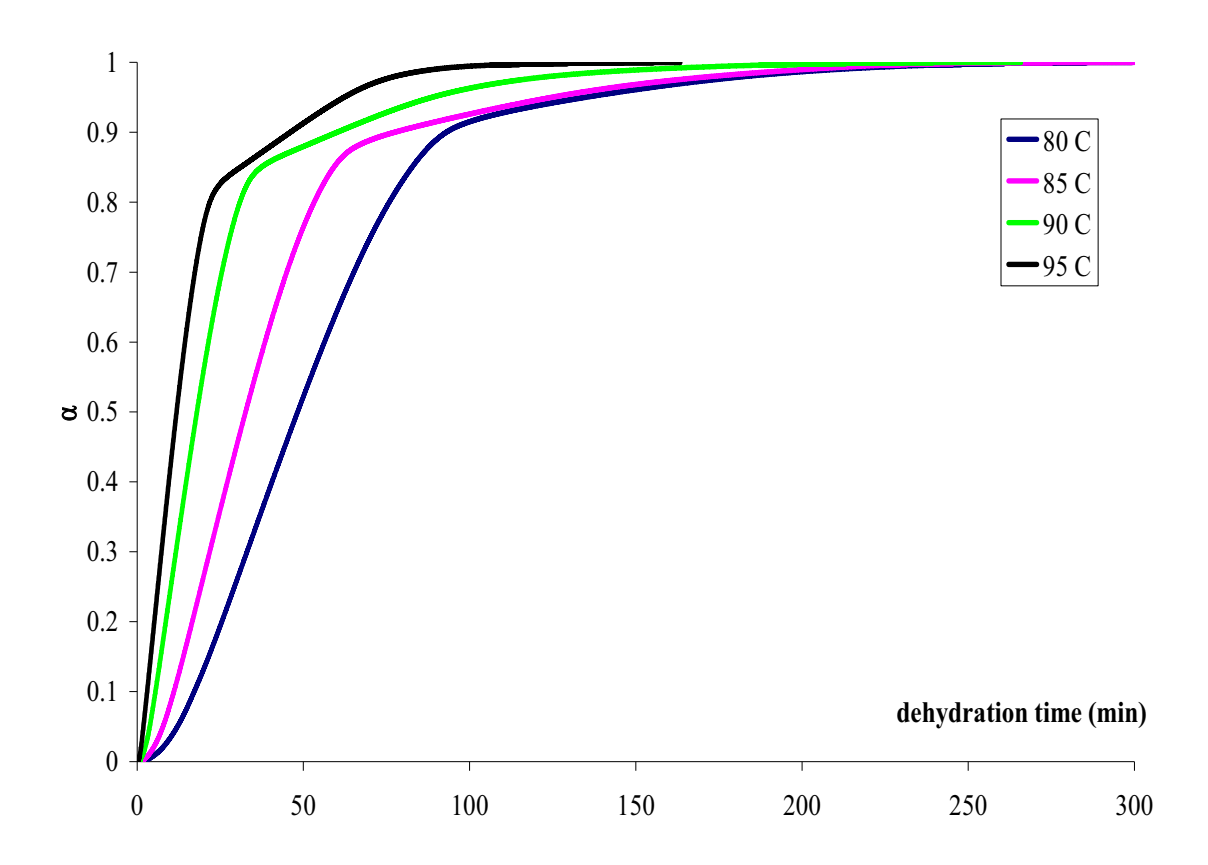


Figure 23  $\,$   $\alpha$ -t curves of dehydration of hemipentahydrate NF at different  $T_{iso}$ 



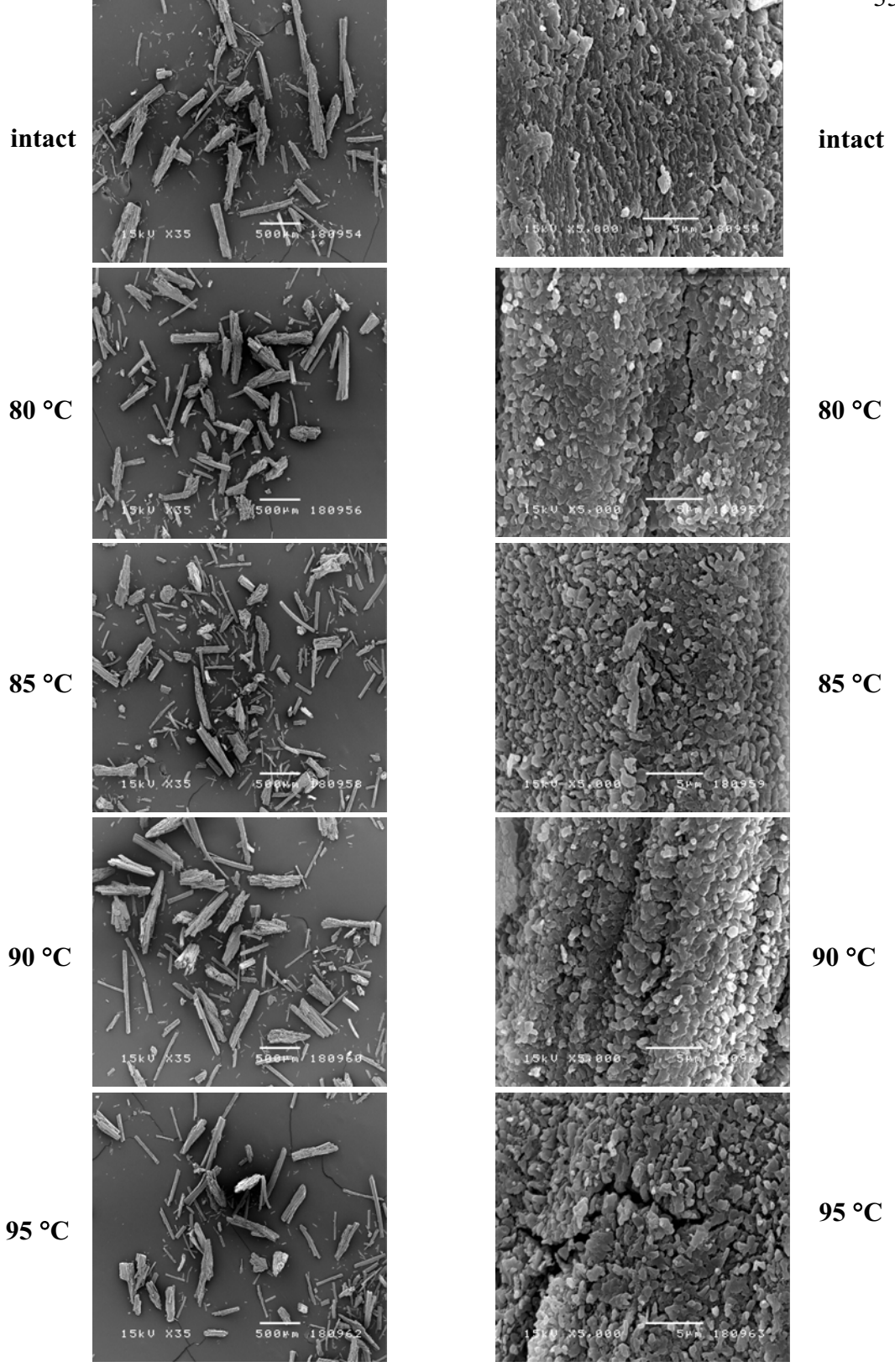


Figure 24 SEM photomicrographs of hemipentahydrate NF after complete dehydration at various  $T_{iso}$  (left column at the magnification of 35, right column at the magnification of 5000)

Table 3 The activation energy of isothermal dehydration of hemipentahydrate NF with various solid state kinetic models

	E <sub>a</sub> (kJ/mol)		
Model equation	First step of dehydration	Second step of dehydration	
	(0.20 to 0.80 of $\alpha$ )	(0.93 to 0.97 of $\alpha$ )	
Avrami Eroféev			
1 dimensional	76.56	119.23	
2 dimensional	75.84	119.19	
Phase Boundary			
2 dimensional	76.95	120.45	
3 dimensional	77.22	121.10	

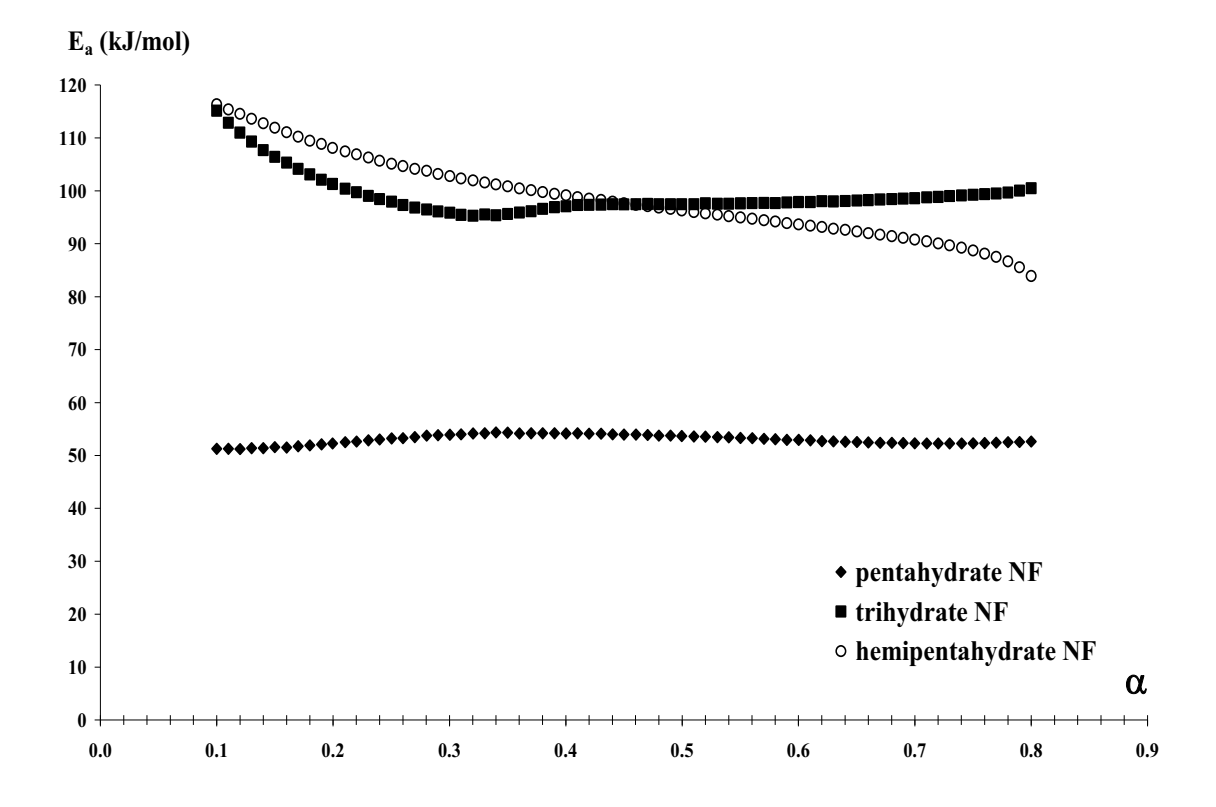


Figure 25 Comparative activation energy of dehydration derived from model independent solid state kinetic of different stoichiometric NF hydrates

## Isothermal Dehydration of Trihydrate NF and Pentahydrate NF

Due to a complex dehydration behavior of trihydrate NF and pentahydrate NF, IDSC of both hydrate NF (Figure 26 and Figure 27) showed consecutive dehydration similar to hemipentahydrate NF. However, these behaviors showed clearer separation between two phases of dehydration than that of hemipantahydrate NF. The  $T_{iso}$  of trihydrate NF and pentahydrate NF at different  $T_{iso}$  were able to be elucidated as two points. The first  $T_{iso}$  was selected between the first and second dehydration endotherm while the second  $T_{iso}$  was the time of unchanged power of later dehydration phase in IDSC thermogram. In this study, the  $T_{iso}$  of first step dehydration for trihydrate NF were 310, 180, 110 and 80 mins while the  $T_{iso}$  of second step or complete dehydration were 750, 510, 330 and 210 mins at 80  $^{\circ}$ C, 85  $^{\circ}$ C, 90  $^{\circ}$ C and 95  $^{\circ}$ C, respectively. On the other hand, the first  $T_{iso}$  of pentahydrate NF were 240, 140, 90, 70 mins and the second  $T_{iso}$  for complete dehydration were 600, 390, 330, 240 mins at 80  $^{\circ}$ C, 85  $^{\circ}$ C, 90  $^{\circ}$ C and 95  $^{\circ}$ C, respectively. The direct energy measurement of the first and the second steps (complete dehydration) were determined and tabulated in Tables 4 and 5. Additional data of residual water content and particle size of each dehydrated sample were also included in these tables.

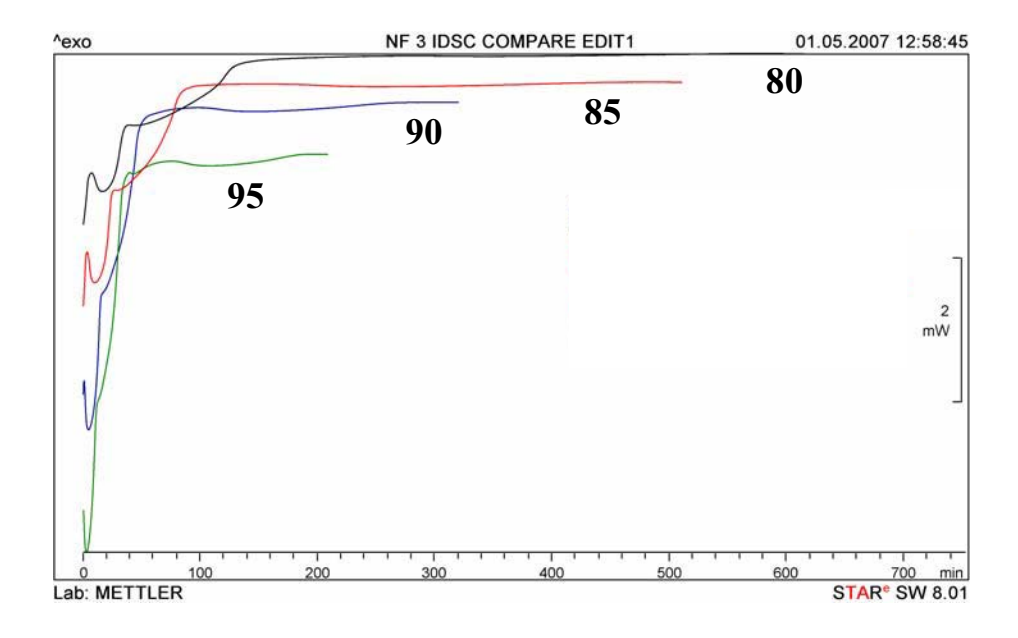


Figure 26 IDSC thermograms of trihydrate NF during isothermal dehydration at various T<sub>iso</sub>

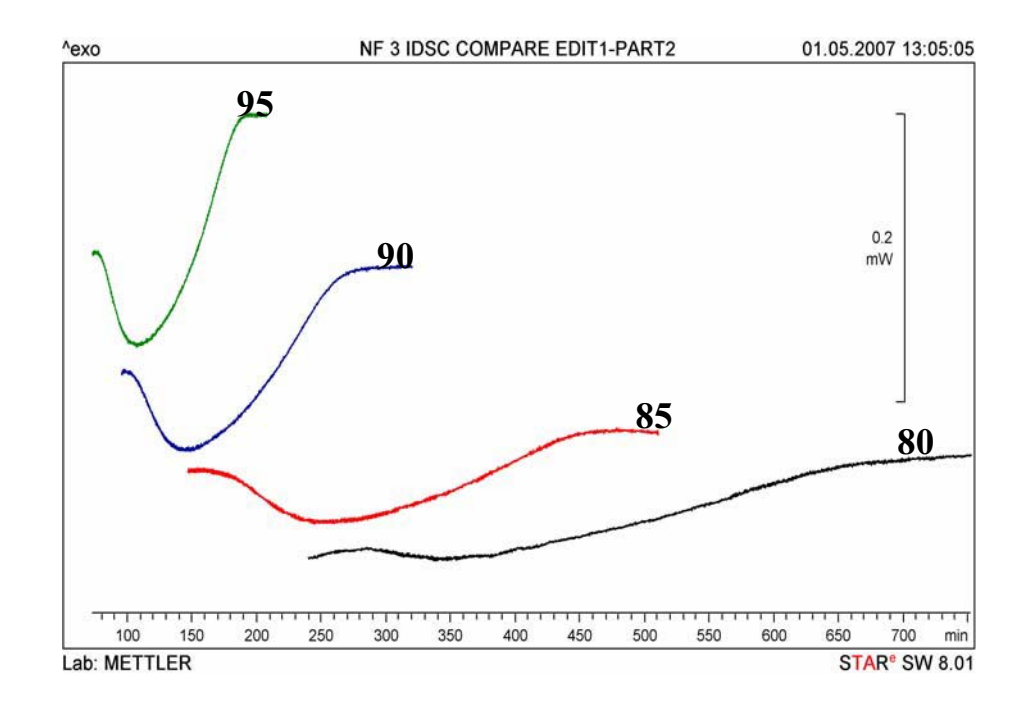


Figure 26 (cont.) IDSC of the second step of the thermograms obtained from trihydrate NF during isothermal dehydration at various  $T_{\rm iso}$ 

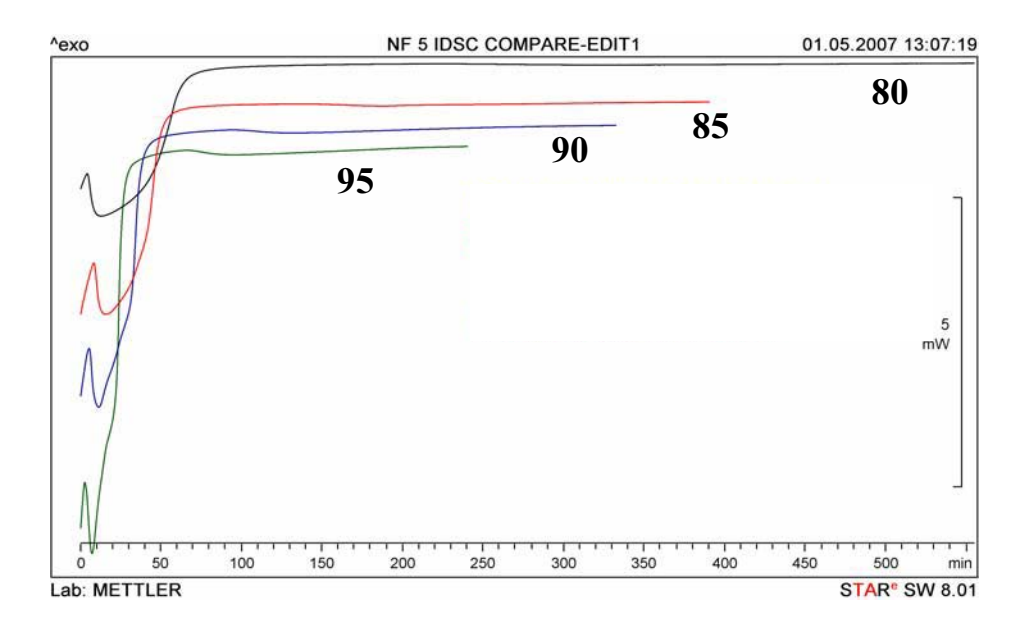


Figure 27 IDSC thermograms of pentahydrate NF during isothermal dehydration at various  $\rm T_{\rm iso}$ 

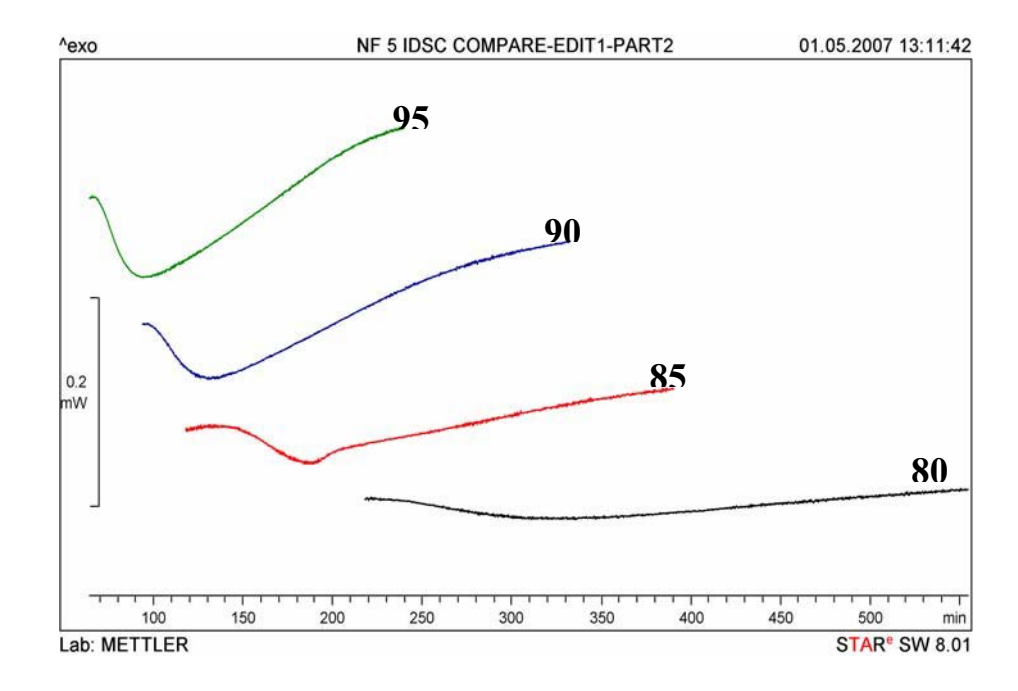


Figure 27 (cont.) IDSC of the second step of the thermograms obtained from pentahydrate NF during isothermal dehydration at various  $T_{\rm iso}$ 

Table 4 Dehydration energy, residual water content and particle size of dehydrated trihydrate NF after dehydration at different  $T_{\rm iso}$ 

Step of	$T_iso$	Dehydration	Residual water content	d [v,0.5]
dehydration	(°C)	energy (J/g)	by TGA (% w/w)	(micron)
Intact form	-	-	14.88 ± 0.08	241.71 ± 1.95
First step	80	375.46 ± 17.78	$3.03 \pm 0.42$	227.58 ± 4.66
	85	379.73 ± 10.21	2.64 ± 0.21	235.53 ± 2.97
	90	374.73 ± 2.34	2.91 ± 0.40	231.67 ± 2.27
	95	360.74 ± 4.16	$3.43 \pm 0.09$	236.13 ± 1.39
Complete	80	455.38 ± 7.56	0.56 ± 0.35	234.86 ± 2.17
dehydration	85	436.29 ± 42.09	$0.36 \pm 0.16$	215.09 ± 3.89
step	90	435.82 ± 18.74	0.11 ± 0.01	229.81 ± 0.35
	95	436.57 ± 3.87	0.15 ± 0.07	228.65 ± 2.13

Table 5 Dehydration energy, residual water content and particle size of dehydrated pentahydrate NF after dehydration at different  $T_{\rm iso}$ 

Step of	T <sub>iso</sub>	Dehydration	Residual water content	d [v,0.5]
dehydration	(°C)	energy (J/g)	by TGA (%w/w)	(micron)
Intact form	-	-	20.87 ± 0.15	211.04 ± 1.46
First step	80	409.32 ± 3.18	3.09 ± 0.08	199.52 ± 0.99
	85	392.63 ± 11.20	2.75 ± 0.17	198.91 ± 2.23
	90	387.12 ± 9.86	3.47 ± 0.19	168.52 ± 2.19
	95	400.25 ± 16.29	2.62 ± 0.15	203.14 ± 2.75
Complete	80	416.59 ± 21.18	1.09 ± 1.16	205.58 ± 1.84
dehydration	85	436.90 ± 12.96	$0.72 \pm 0.30$	187.77 ± 1.64
step	90	434.50 ± 13.96	0.73 ± 0.12	197.51 ± 1.75
	95	448.12 ± 11.16	0.75 ± 0.01	192.52 ± 3.76

The direct energy measurement within each group of dehydration step with respect to temperatures used for T<sub>iso</sub> for trihydrate NF and pentahydrate NF were insignificantly different. However, the differences of the energies between the first step dehydration and the complete step of dehydration for trihydrate NF and pentahydrate NF were statistically found (p<0.05). The results revealed that the total required energy for complete dehydration of both hydrates NF were not affected by the temperatures used similar to hemipentahydrate NF. The residual water contents of both trihydrate NF and pentahydrate NF after the first step of dehydration was approximately 2.5-3.5% w/w (Tables 4 and 5), indicating an incomplete dehydration of both hydrates after the first step of dehydration. Furthermore, XRPD patterns of both dehydrated trihydrate NF (Figure 28) and pentahydrate NF (Figure 29) after the first step of dehydration shown to be a mixture of anhydrous NF Form A and the hydrated transitional phase. However, only anhydrous NF Form A was found after allowing the complete dehydration for both NF hydrates (Figures 30 and 31). The low level of residual water contents of trihydrate NF and pentahydrate NF were at or below 1% w/w after the complete dehydration and confirmed the conversion to anhydrous NF Form A.

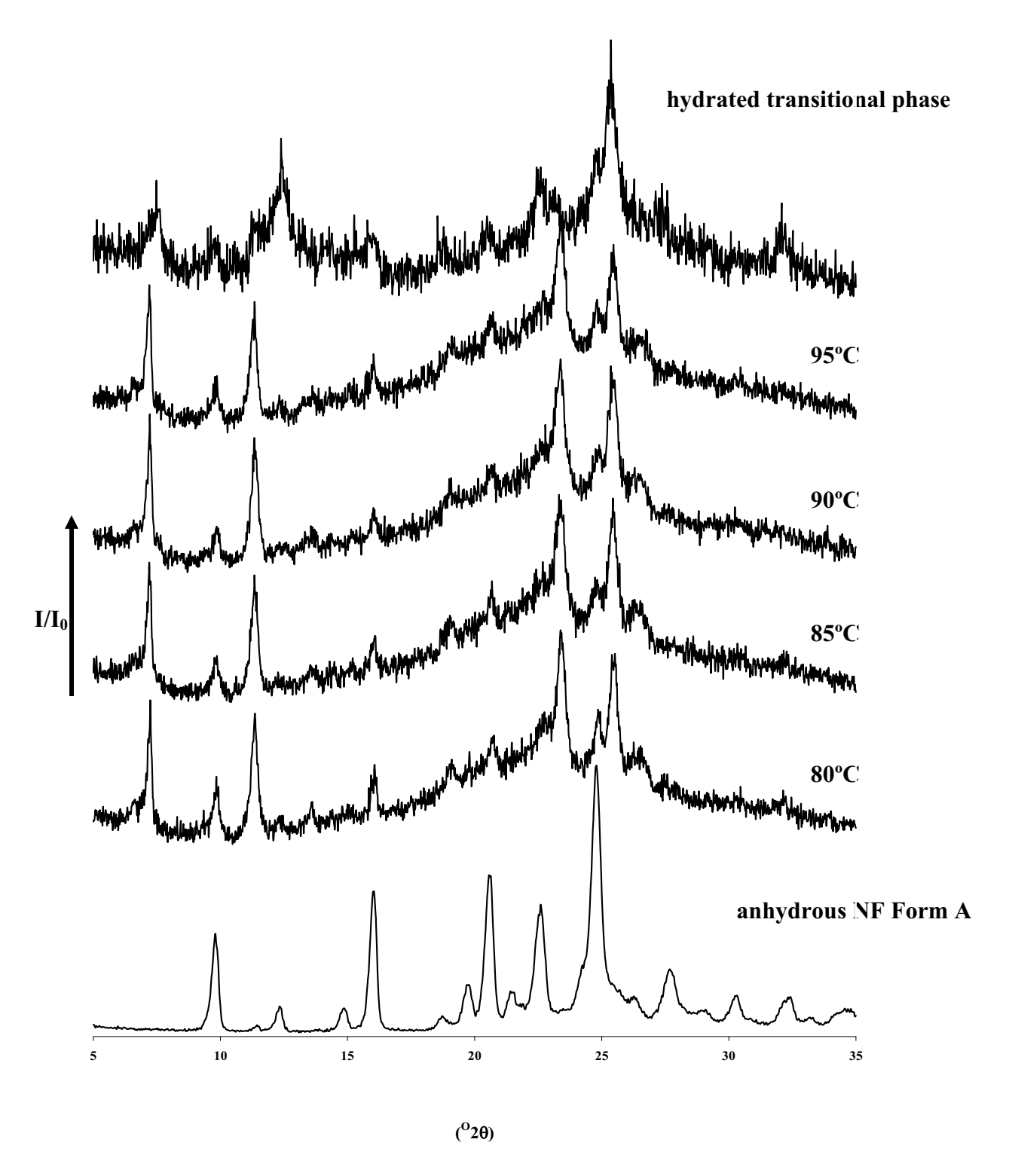


Figure 28 XRPD diffractograms of dehydrated trihydrate NF after first step of isothermal dehydration with respect to  $T_{\rm iso}$ 

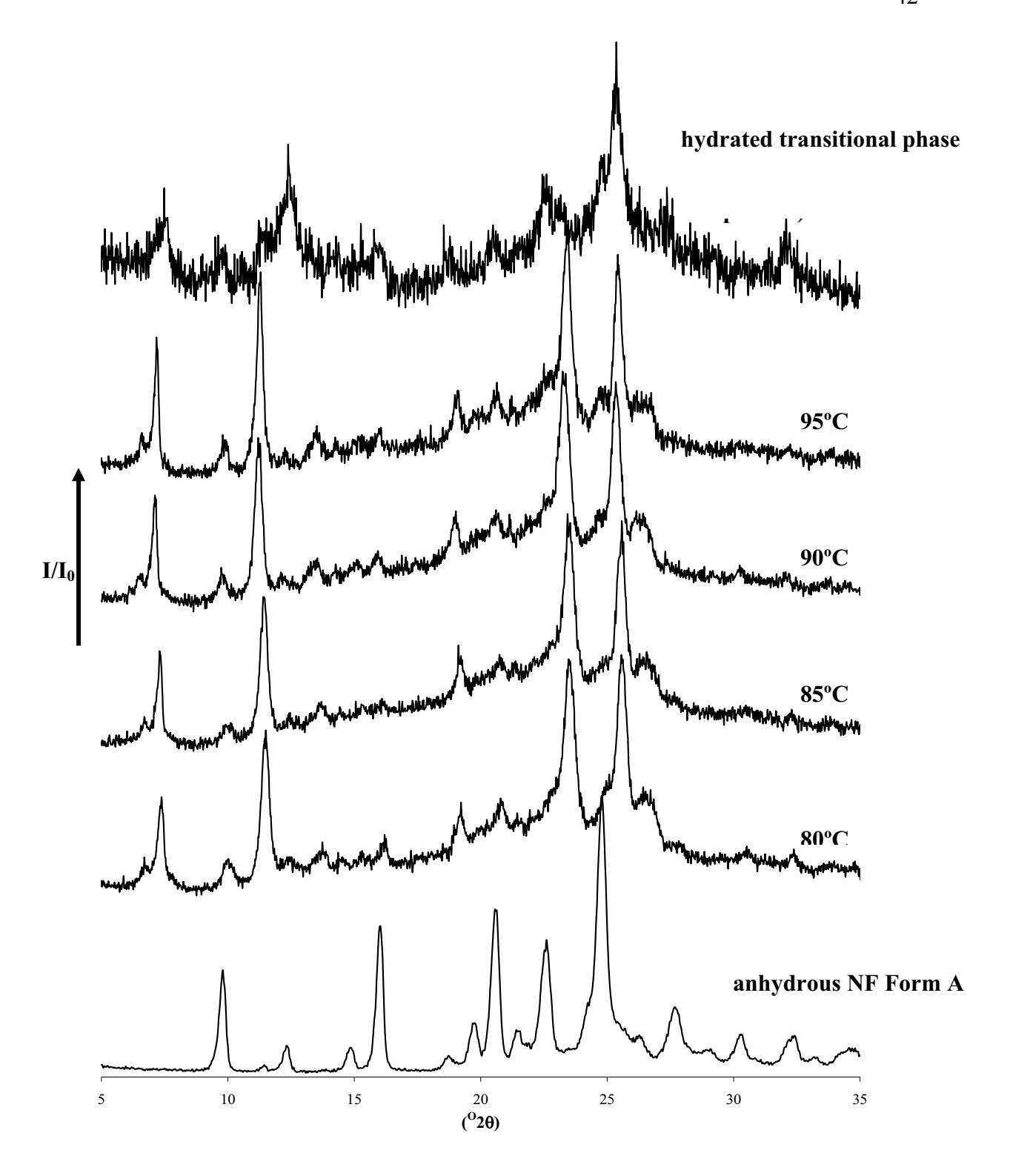


Figure 29 XRPD diffractograms of dehydrated pentahydrate NF after first step of isothermal dehydration with respect to  $\mathsf{T}_{\mathsf{iso}}$ 

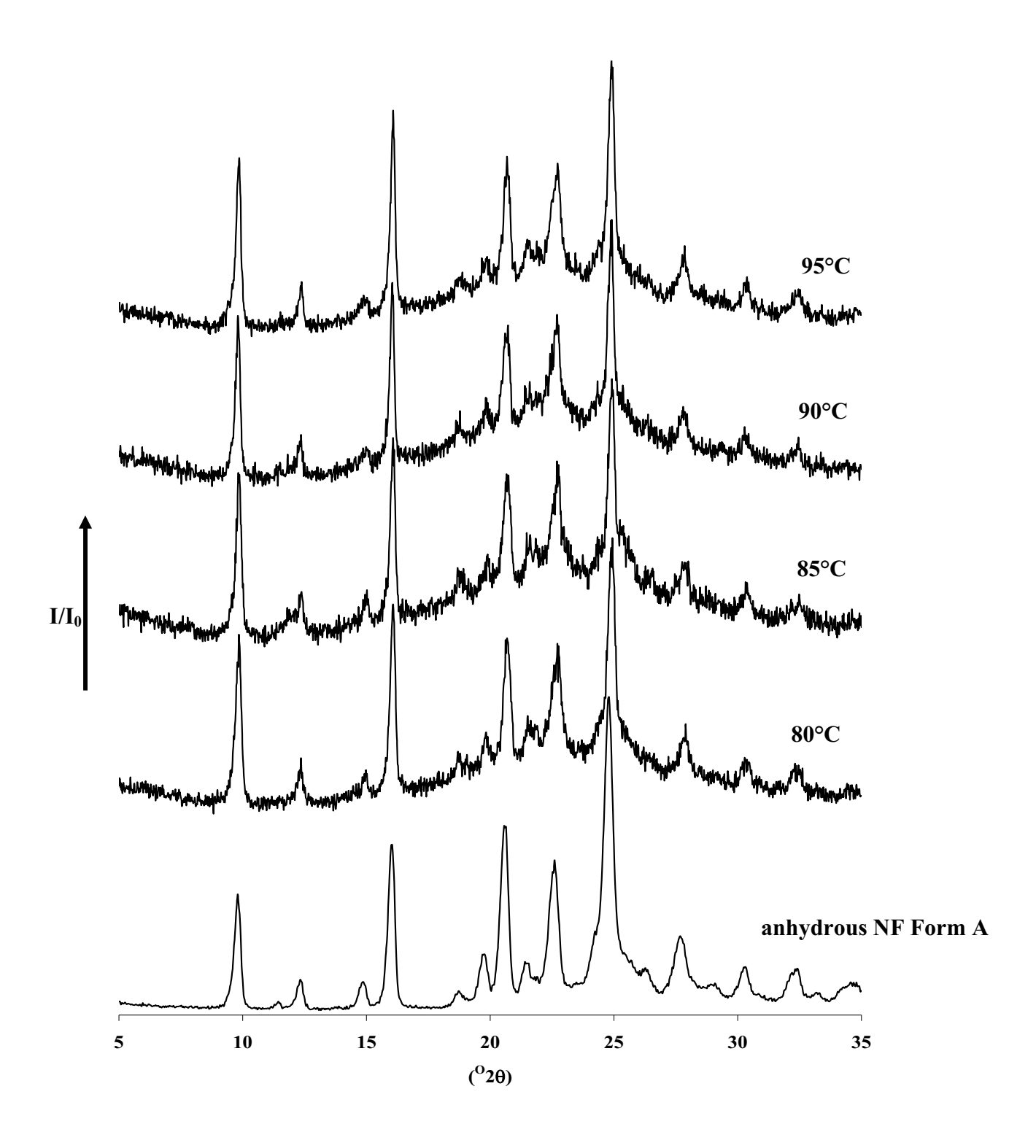


Figure 30 XRPD diffractograms of dehydrated trihydrate NF after complete dehydration with respect to  $T_{\rm iso}$ 

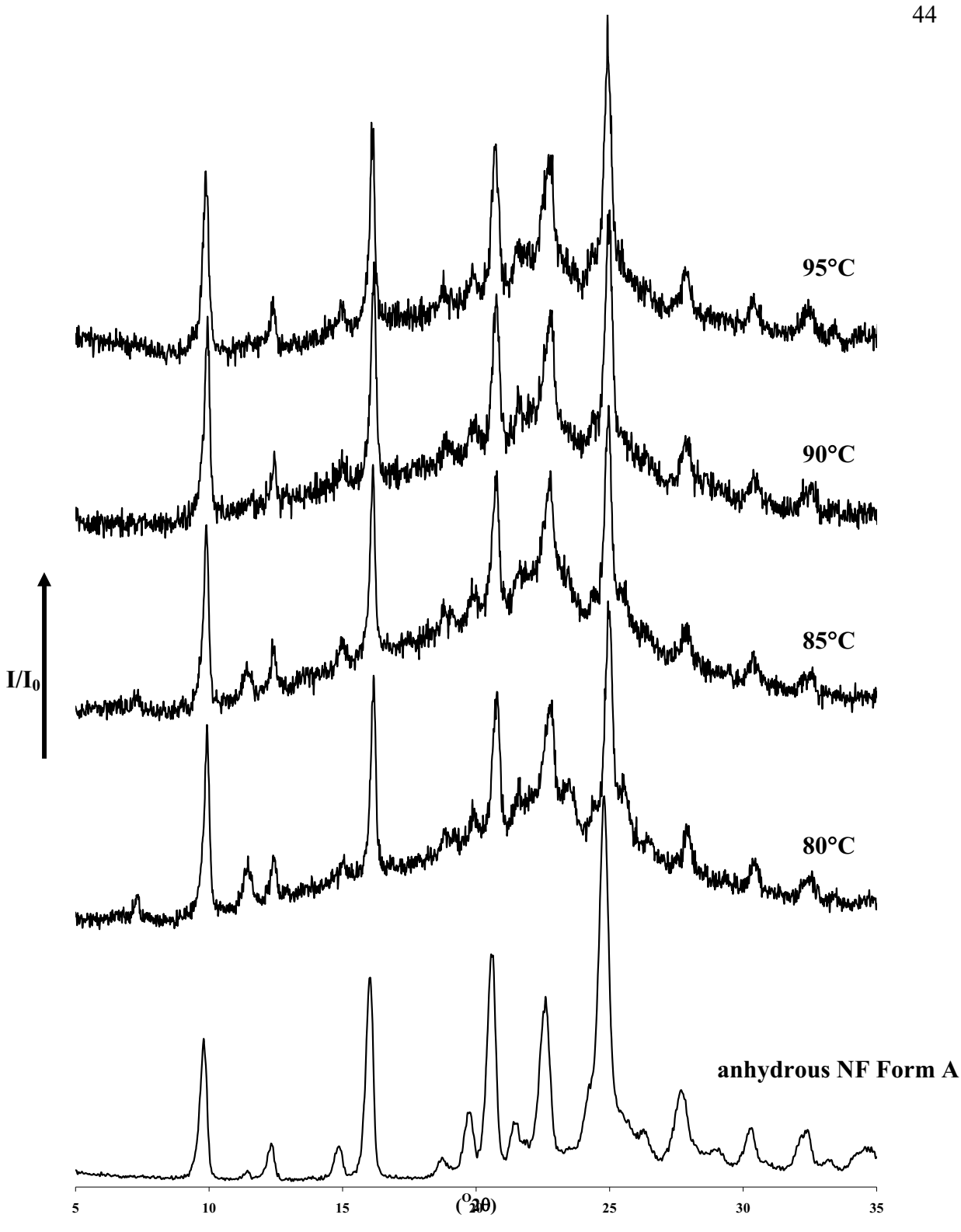


Figure 31 XRPD diffractograms of dehydrated trihydrate NF after complete dehydration with respect to  $T_{\text{iso}}$ 

The particle size of dehydrated trihydrate NF and dehydrated pentahydrate NF were different from the particle size of intact form. However, these findings could not be concluded that particle size reduction of trihydrate NF and pentahydrate NF were clearly seen after dehydration. Because the maximum magnitude of particle size reduction of trihydrate NF and pentahydrate NF were approximately 25 microns and 40 microns, respectively. In summary, thermal dehydration could not reduce the particle size to a significant level for both trihydrate NF and pentahydrate NF.

Although thermal dehydration could not generate small particles of trihydrate NF and pentahydrate NF, the disruption of crystal took place as shown in SEM photomicrographs. Dehydration of trihyhydrates NF and pentahydrate NF with different steps of dehydration showed cracks on the surface of particles (Figures 32 - 35) but it could not promote the individually scattered small particles as seen in BDM. However, the defects seen on large particles may potentially generate small particles with the manipulation of only very mild mechanical force. For example, mild pulverizing of deammoniated methabarbital gave the small particle than intact methabarbital (Sekiguchi et al., 1984).

The relationship between fraction reacted (Q) and dehydration time (t) of trihydrate NF and pentahydrate NF are presented in Figures 36 and 37, respectively. In the case of trihydrate NF, the dehydration reaction may be separated in three steps due to unequal slopes whereas two different slopes were determined for the dehydration of pentahydrate NF. In term of model dependent kinetics, the Ea of each defined dehydration steps of trihydrate NF and pentahydrate NF are presented in Tables 6 and 7, respectively. Model dependent approach gave Ea of the dehydration of trihydrate NF of approximately 80 J/g, 98 J/g and 94 J/g for first, second and third step of dehydration, respectively. These results revealed that the "rate" of dehydration of all three steps were considered to be temperature dependent and the magnitude of dehydration rate dependent on temperature were similar. Meanwhile model independent approach showed the value of Ea of 85-115 kJ/mol which are similar to the energy barriers of each step of dehydration (Figure 24). The Ea from model independent of trihydrate NF showed initial decrease and gradually increased at later step of dehydration. It indicated the reduction of energy barrier due to the partially disrupted structure. However, the structure integrity was regenerated at the later stage seen from an increase of E<sub>a</sub>. Thus, destroyed structure of trihydrate NF during partial dehydration supported the particle size reduction even the stable structure later exists. For pentahydrate NF, model dependent showed E<sub>a</sub> of dehydration at approximately 50 J/g, 70-90 J/g for early and later step of dehydration, respectively. These data were different from the data

obtained with trihydrate NF. It indicated that the magnitude of temperature dependency in early step was lower than that of the later step of dehydration. Thus, the rate of dehydration of pentahydrate NF at early phase changed did not depend wholly on the dehydration temperature was raised equally. On the other hand, the  $E_a$  of pentahydrate NF from model independent, 50 kJ/mol, was equal to the  $E_a$  obtained from the early step of dehydration by model dependent. Moreover, the pattern of the change of  $E_a$  over the  $\Omega$  of 0.1 to 0.8 was negligible changed. It should provide the stable structure and unchanged particle size of pentahydrate NF after dehydration. However, the particle size reduction of pentahydrate NF experimentally occurred. Hence, it should have other controlled factors of the particle size reduction of pentahydrate NF upon heating.

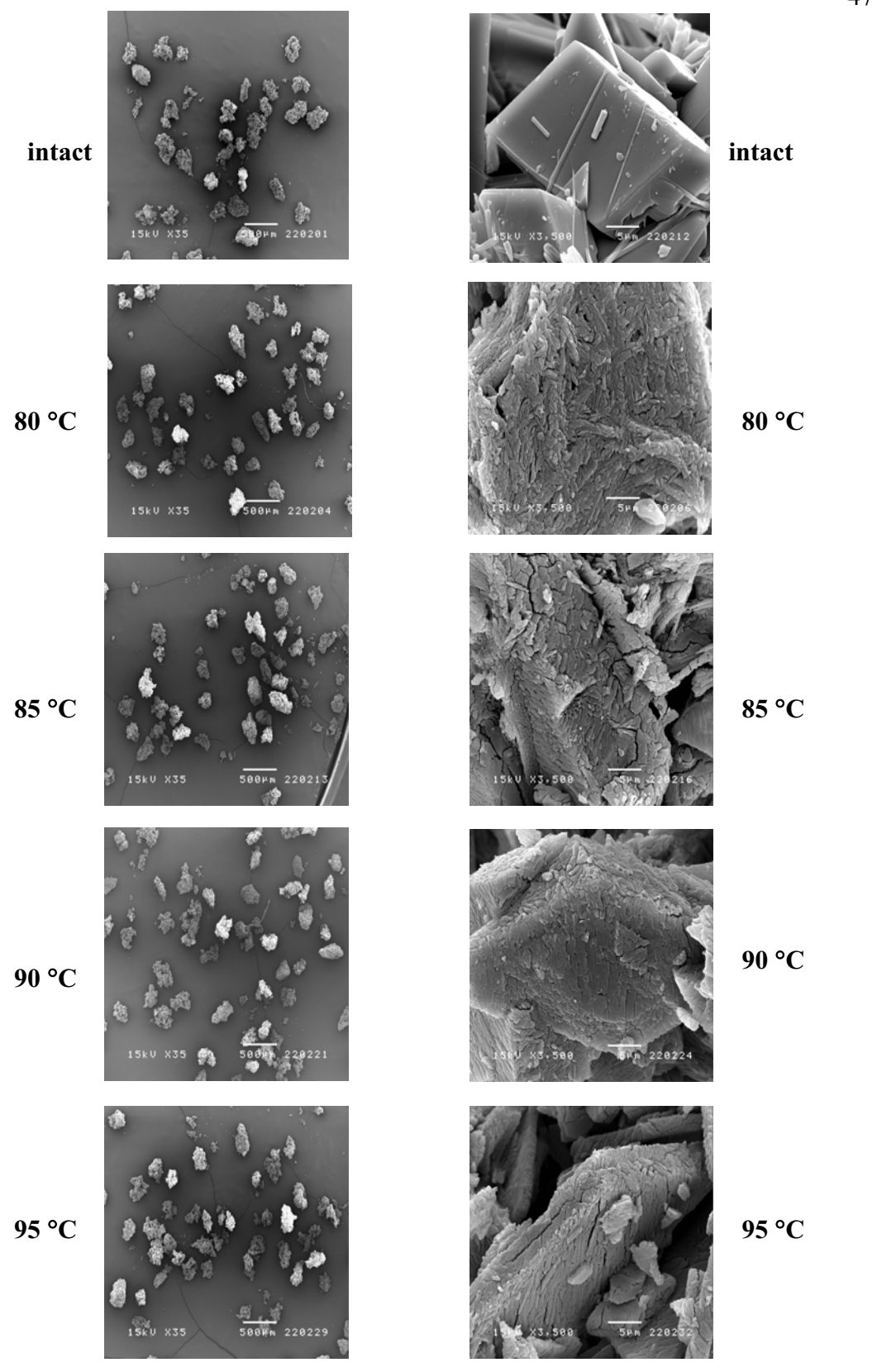


Figure 32 SEM photomicrographs of dehydrated trihydrate NF during isothermal dehydration after the first dehydration step with respect to  $T_{iso}$  (left column at the magnification of 35, right column at the magnification of 3500)

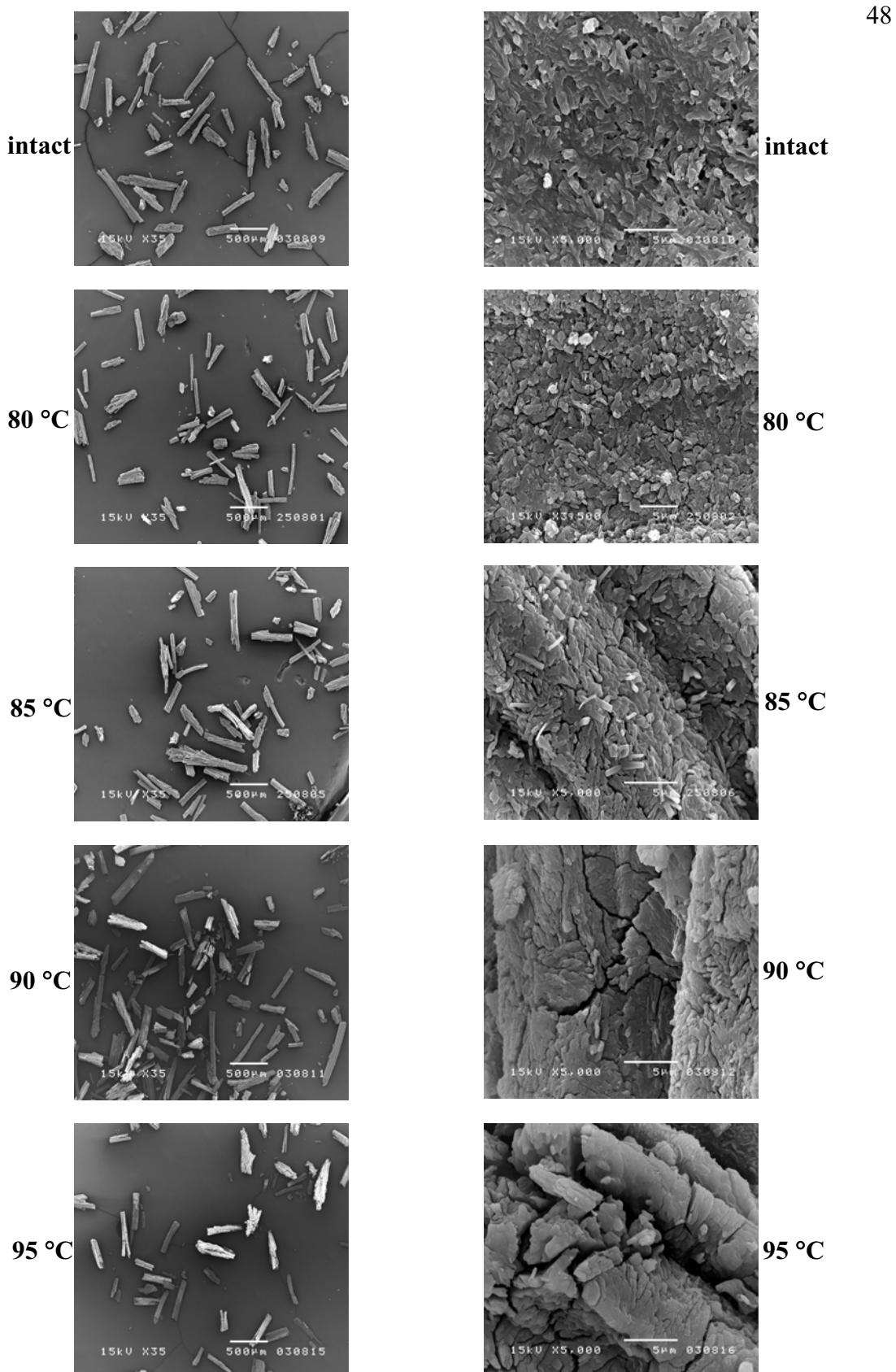


Figure 33 SEM photomicrographs of dehydrated pentahydrate NF during isothermal dehydration after the first dehydration step with respect to  $T_{\rm iso}(\mbox{left column}$  at the magnification of 35, right column at the magnification of 5000 except of 80°C at 3500)